

Martina Strempl, BSc

Influence of the TORC1 pathway on early ribosome biogenesis in yeast

MASTER'S THESIS

to achieve the university degree of

Master of Science

Master's degree programme: Molecular Microbiology

submitted to

Graz University of Technology

Supervisor

Ao. Univ.-Prof. Mag. Dr. Helmut Bergler

Institute of Molecular Biosciences

AFFIDAVIT

I declare that I have authored this thesis independently, that I have not used other than the declared sources/resources, and that I have explicitly indicated all material which has been quoted either literally or by content from the sources used. The text document uploaded to TUGRAZonline is identical to the present master's thesis.

12.04.2019

Date

Martina Strempl

Signature

An dieser Stelle möchte ich all jenen danken, die durch ihre fachliche und persönliche Unterstützung zum Gelingen dieser Arbeit beigetragen haben.

Mein besonderer Dank gilt Herrn Ao. Univ.-Prof. Mag. Dr. Helmut Bergler, der mir die Arbeit an diesem Projekt nicht nur ermöglicht, sondern mich auch hervorragend betreut und durch hilfreiche Anregungen und Ideen durch dieses spannende Thema gleitet hat.

Herzlich bedanken möchte ich mich auch bei Lisa Kofler und Magdalena Gerhalter, ohne deren Hilfe und Bemühungen diese Arbeit nicht zustande gekommen wäre, sowie bei Gertrude Zisser für ihre stetige Hilfsbereitschaft und für die vielen tollen Tipps.

Weiterhin danke ich der gesamten „Ribosomen-Crew“, die mich so herzlich in ihre Mitte aufgenommen und die mir eine unvergessliche Zeit bereitet hat.

Ein besonderer Dank gilt meiner Familie, insbesondere meinen Eltern Gertrude und Werner, die mich auf meinem Weg durch das Studium begleitet und mir dieses auch ermöglicht haben.

Ich danke Christoph, der immer ein offenes Ohr für meine Probleme hat, und in der Zeit der Erstellung dieser Arbeit für mich da war.

Schließlich danke ich meinen Freunden für die schöne Studienzeit in Graz.

Zusammenfassung

TORC1 (*Target Of Rapamycin Complex 1*) ist eine konservierte, Nährstoff-sensitive Serin/Threoninkinase, die als zentraler Regulator des Zellwachstums fungiert. Ihre Kinaseaktivität kann durch das antimykotische Medikament Rapamycin, einem natürlichen Metaboliten mehrerer Actinomyceten, gehemmt werden. Der Wirkstoff bildet einen Komplex mit dem FK506-Bindeprotein (FKBP), der dann in der Lage ist, nahe der katalytisch aktiven Domäne der TORC1-Komponente Tor1 zu binden.

Ziel dieser Arbeit war die Untersuchung der Auswirkungen der TORC1-Kinase auf die Ribosomenbiogenese der Bäckerhefe *Saccharomyces cerevisiae*. Die Behandlung mehrerer Stämme mit Rapamycin zeigte, dass in Gegenwart des Wirkstoffes das primäre rRNA-Transkript, die 35S Prä-rRNA, überwiegend an der A₃-Site anstelle der A₂-Site geschnitten wird. Dies deckt sich mit vorangegangenen Daten von Kos-Braun et al., 2017. Um die Auswirkungen auf Protein- und rRNA-Gehalt zu bestimmen, wurden ausgewählte nucleolare Prä-Ribosomen von verschiedenen Reifungsstadien (Nop58-, Noc2-, Nog1- und Nsa1-Partikel) mittels Tandem Affinity Purification (TAP) isoliert und mittels Western- und Northern Blotting analysiert. Diese Analyse zeigte spezifische Änderungen der prä-ribosomalen Partikelkomposition. Nop58-Partikel zeigten, dass Nop58 und Nop1, zwei Box C/D snoRNP (*small nucleolar ribonucleoprotein*) Kernproteine, an der 23S rRNA zurückgehalten wurden. Das Noc2-Partikel aus dem Rapamycin behandelten Stamm wies außerdem Charakteristika eines späteren prä-ribosomalen Komplexes, dem die 27SA₂ Prä-rRNA fehlte, der aber reich an 27SA₃ und/oder 27SB rRNA war, auf. Diese Veränderungen im Noc2-Partikel waren TORC1-spezifisch, da die Prä-rRNA eines Rapamycin-resistenten Stammes auch in Gegenwart des Wirkstoffes an der A₂-Site geschnitten wurde. Zusätzlich konnte eine Beeinflussung der Prä-rRNA- und Protein-Zusammensetzung von Prä-Ribosomen durch spezifische *TOR1*-Mutationen nachgewiesen werden. Weitere Untersuchungen erlaubten Rückschlüsse auf mögliche Targets des TORC1-Pathways in der Ribosomenbiogenese.

Insgesamt bietet diese Arbeit erstmalig einen Einblick in die individuellen Veränderungen in der Zusammensetzung früher prä-ribosomaler Komplexe nach TORC1-Inaktivierung.

Abstract

The Target Of Rapamycin Complex 1 (TORC1) is a conserved, nutrient-sensitive serine/threonine kinase that acts as a central regulator of cell growth. The kinase activity of TORC1 can be inhibited by the drug rapamycin, which is a natural metabolite produced by several actinomycetes. It forms a complex with the FK506-binding protein (FKBP), which is able to bind near the catalytically active domain of the TORC1 component Tor1.

This study aimed to investigate the impact of the TORC1 kinase on ribosome assembly in the baker's yeast *Saccharomyces cerevisiae*. Treatment of several strains with rapamycin demonstrated that in the presence of the drug, the rRNA primary transcript, the 35S pre-rRNA, is predominantly cleaved at the A₃ site instead of at the A₂ site. This is consistent with previous data shown by Kos-Braun et al., 2017. Selected nucleolar pre-ribosomes from different maturation steps (Nop58-, Noc2-, Nog1- and Nsa1-particles) were isolated via tandem affinity purification (TAP) and analysed by western and northern blotting in order to determine the effects of the inhibitor on their protein and rRNA content. Changes in the pre-ribosomal particle composition upon inhibitor treatment were unique for each of the nucleolar pre-ribosomal particle. For instance, Nop58-particles showed an entrapment of the box C/D small nucleolar ribonucleoproteins (snoRNPs) Nop58 and Nop1 at 23S rRNA. In contrast, the Noc2-particle shifted to a later pre-ribosomal complex, lacking 27SA₂ pre-rRNA, but accumulating 27SA₃ and/or 27SB pre-rRNA after rapamycin treatment. These changes in Noc2-particles were TORC1-specific, as the pre-rRNA of a rapamycin resistant strain was cleaved at A₂ in the presence of the drug. These results underline the importance of the TORC1 pathway for the regulation of ribosome biogenesis which is further supported by pronounced compositional changes of pre-ribosomal particles from Tor1 mutant strains observed in this study. Further investigations suggested possible targets of the TORC1 pathway in ribosome biogenesis.

Taken together, this thesis provides, for the first time, insight into the individual changes in the composition of early pre-ribosomal complexes upon TORC1 inactivation.

Table of Contents

1	Introduction.....	6
1.1	Ribosomal biogenesis: An overview of the maturation of pre-ribosomal particles.....	6
1.2	Tor, a component of the TORC1 complex, is inhibited by rapamycin.....	8
1.3	TORC1 influences ribosomal biogenesis.....	10
1.4	Role of the early assembly factors Nop58 and Noc2 in TORC1 pathway and in ribosomal biogenesis.....	13
2	Material and Methods.....	16
2.1	<i>Saccharomyces cerevisiae</i> strains and media.....	16
2.2	TAP tagging of <i>NOC2</i>	18
2.3	Tandem affinity purification (TAP)	22
2.4	Western blot analysis of TEV eluates	24
2.5	Northern blot analysis of CEs and TAP-purified samples	27
2.6	Fluorescence Microscopy.....	30
3	Results	31
3.1	Effect of Rapamycin on rRNA and protein levels of Nop58-particles	31
3.2	Effect of Rapamycin on the composition of the Noc2-particle	34
3.3	Impact of hyperactive <i>tor1^{L2134M}</i> variant on pre-ribosomal particle composition	36
3.4	TORC1 inactivation does not influence Noc2 localisation.....	37
3.5	Effects of TORC1 inhibition on intermediate and in late nucleolar pre-ribosomal particles	38
3.6	There are serine-phosphorylated proteins in Nop58-, Noc2-, Nog1- and Nsa1-particles	41
3.7	Subcellular localisation of late nucleolar pre-60S assembly factors in the absence and presence of rapamycin	46
4	Discussion	48
4.1	Particle-specific compositional changes after long-term treatment with rapamycin	48
4.2	Role of selected factors in ribosomal biogenesis, which were shown to be affected after short-term treatment with rapamycin.....	50
5	References.....	54

1 Introduction

1.1 Ribosomal biogenesis: An overview of the maturation of pre-ribosomal particles

Ribosomes are the "protein factories" of any cell. They are responsible for the translation of genetic information into the amino acid sequences of proteins. Eukaryotic 80S ribosomes contain two subunits, one small or 40S and one large or 60S subunit. The core of each subunit is formed by ribosomal RNA (rRNA). In addition, each subunit contains its own set of ribosomal proteins (r-proteins), which are mainly located on the surface. Functionally, the 40S subunit is responsible for the association of transfer RNAs (tRNAs) and messenger RNAs (mRNAs); whereas the 60S subunit contains the peptidyl transferase centre, which is necessary for the formation of peptide bonds between amino acids. *Saccharomyces cerevisiae* ribosomes consist of 4 rRNAs (5S, 5.8S, 18S and 25S) and 79 r-proteins in total (Woolford and Baserga, 2013). The biogenesis of its subunits is described in the following paragraphs and schematically shown in Figure 1.

Ribosomal DNA (rDNA) exists in a pool of about 150 tandem repeats of transcription units, which form the nucleolus, a non-membrane-bound subcompartment of the nucleus. Transcriptionally active units serve as a template for the synthesis of the 35S primary pre-rRNA transcript by RNA polymerase I (RNAPI) and for the synthesis of 5S pre-rRNA by RNA polymerase III (RNAPIII). The 35S primary transcript contains the sequences for the mature 18S, 5.8S and 25S rRNA. These sequences are separated by external (5'ETS and 3'ETS) and internal transcribed spacers (ITS1 and ITS2). Those spacers are then removed through several processing steps occurring in the nucleolus (reviewed in more detail in Fernández-Pevida et al., 2015). rRNA processing and r-protein binding requires more than 200 assembly factors (AFs) and 76 small nucleolar RNAs (snoRNAs), which are not present in the mature subunits. The assembly factors are *trans*-acting proteins with distinct biochemical functions. For example, they include ATPases, GTPases, helicases, methyltransferases, nucleases and scaffold proteins. At different stages of ribosomal assembly, various AFs and snoRNAs are associated with pre-rRNAs and r-proteins. Therefore, heteromorphic pre-ribosomal particles can be distinguished by their protein and RNA content (Konikkat and Woolford, 2017).

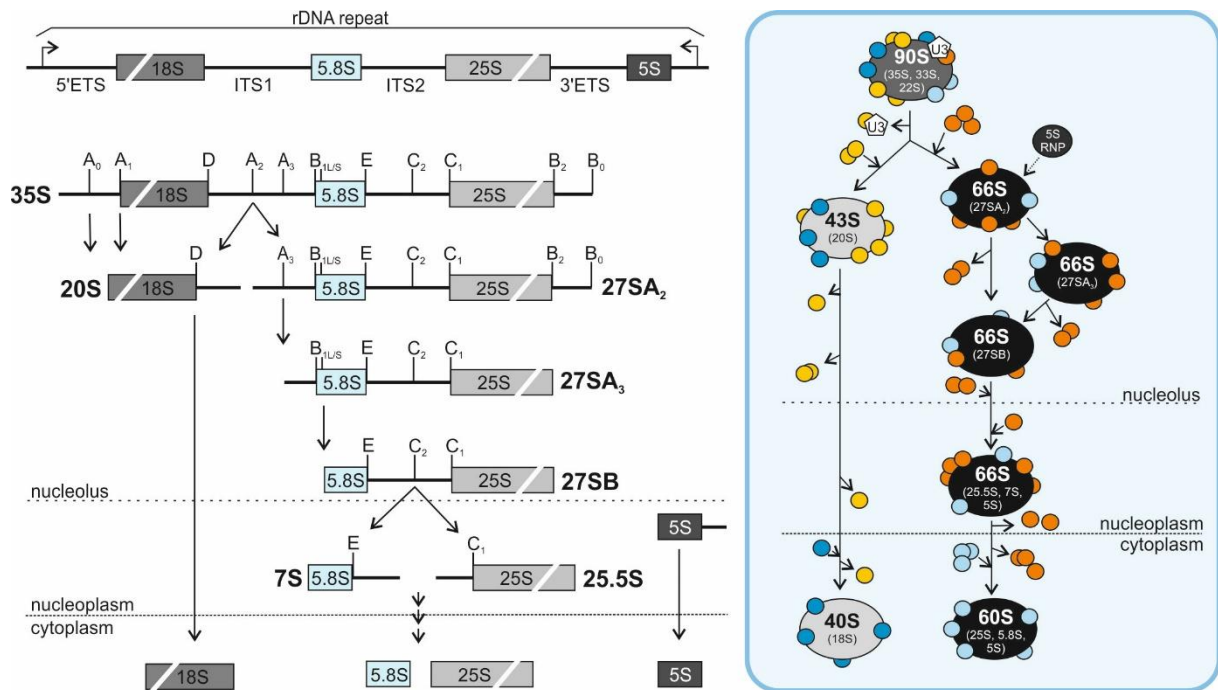


Figure 1: Maturation pathway of yeast ribosomes. Left: Major pathway of pre-rRNA processing. Right: Simplified overview of ribosomal particle assembly. Assembly factors are shown in orange (60S) and yellow (40S), ribosomal proteins in light blue (60S) and dark blue (40S).

Transcription of 35S rDNA starts in the nucleolus. Very early processing steps include the removal of the 5'ETS and the cleavage of the A₂ site, which is located within the ITS1. These events are dependent on the first formed pre-ribosomal particle termed the “small-subunit (SSU) processome” or “90S pre-ribosome” (Fernández-Pevida et al., 2015). The fully assembled particle contains the box C/D U3 snoRNA, at least 18 early binding r-proteins and 51 assembly factors, which are predominantly responsible for the maturation of the small subunit. Thus, the absence of individual 90S factors leads to defects in the 40S subunit assembly (Bernstein et al., 2004; Dragon et al., 2002; Grandi et al., 2002; Zhang et al., 2016).

A₂ cleavage is an important step in rRNA processing as it leads to the separation of the 40S and 60S precursor rRNAs. It has been shown that the segregation of these precursors can occur both post- and co-transcriptionally, but the latter predominates under favourable growth conditions (Kos and Tollervey, 2010; Osheim et al., 2004). It has long been assumed that Rcl1 cuts the A₂ site. But more recent data question this and suggest that the endonuclease Utp24 is responsible for this early cleavage step (Horn et al., 2011; Wells et al., 2016). Regardless, A₂ cleavage creates 20S and 27SA₂ rRNA, which are packaged into 43S and 66S pre-ribosomes, respectively. At this point, the maturation of the 40S and 60S subunits is split into two independent pathways. 43S particles are rapidly transported into the cytoplasm where 20S rRNA is cleaved at the D site to generate mature 18S rRNA. In contrast, the rRNA processing in the 60S subunit is more complex. Further maturation of 27SA₂ rRNA can occur either by the major (85 %) or the minor (15 %) processing pathway (Fernández-Pevida et al.,

2015; Woolford and Baserga, 2013). The major pathway differs from the minor pathway in that the major pathway includes an additional processing step in which the A₃ site is cut through the ribonucleoprotein (RNP) RNase MRP (Lygerou et al., 1996). This results in a further pre-rRNA intermediate, the 27SA₃ rRNA, which is trimmed at the B₁₅ site by exonucleases. In comparison, the creation of 27SB rRNA in the minor pathway proceeds through direct cleavage at the B_{1L} site. Another event in the early 60S subunit maturation is the integration of a ribonucleoprotein complex, which comprises the 5S rRNA. Later processing steps include the removal of the ITS2 by C₂ cleavage and subsequent trimming. Trimming of the resulting 7S and 25.5S intermediates takes place first in the nucleoplasm and then in the cytoplasm, where the last steps of ribosome maturation occurs (Konikkat and Woolford, 2017).

A single *S. cerevisiae* cell harbours about 200000 ribosomes. With a generation time of approximately 100 minutes under optimal conditions, a production of 2000 ribosomes per minute is necessary (Warner, 1999). The formation of ribosomes depends on environmental conditions, and therefore ribosomal biogenesis is strictly regulated. An important regulator of ribosomal biogenesis is the serine/threonine kinase TORC1 (**Target Of Rapamycin Complex 1**), which is highly conserved from yeast to human (reviewed in de la Cruz et al., 2018; Loewith and Hall, 2011).

1.2 Tor, a component of the TORC1 complex, is inhibited by rapamycin

Saccharomyces cerevisiae TORC1 is an approximately 2 MDa sized complex which consists of the four proteins Kog1, Lst8, Tco89 and either Tor1 or Tor2 (Loewith et al., 2002; Reinke et al., 2004). Among them, the phosphatidylinositol kinase-related protein kinases (PIKKs) Tor1 and Tor2 (Helliwell et al., 1994) are the best-studied TORC1 components. Through the isolation of resistant yeast mutants, the Tor proteins were originally discovered as the direct targets of rapamycin in 1991 (Heitman et al., 1991a). Rapamycin (reviewed in Yoo et al., 2017) is a macrocyclic natural product (Figure 2) produced by several actinomycetes, which is known for its growth inhibiting effect on a number of fungi. It forms a complex with the FK506-binding protein (FKBP; encoded by the *FPR1* gene in *S. cerevisiae*) and this complex is then able to bind with (and to thereby inhibit) the Tor proteins (Heitman et al., 1991b, 1991a; Koltin et al., 1991; Lorenz and Heitman, 1995; Stan et al., 1994). Inhibition by rapamycin leads to G1 cell cycle arrest (Heitman et al., 1991a), which is also caused by *TOR1 TOR2* double disruption (Helliwell et al., 1994). How FKBP-rapamycin succeeds in inhibiting the kinase activity of TORC1 is not yet fully understood. It was shown that rapamycin treatment does not inhibit Tor by disruption TORC1 (Loewith et al., 2002). Because the FKBP-rapamycin-binding (FRB) domain is locat-

ed to the kinase domain of Tor (Figure 3), it has been proposed that Tor's kinase activity is suppressed either by direct inhibition and/or by preventing optimal substrate presentation at the catalytic site (Adami et al., 2007).

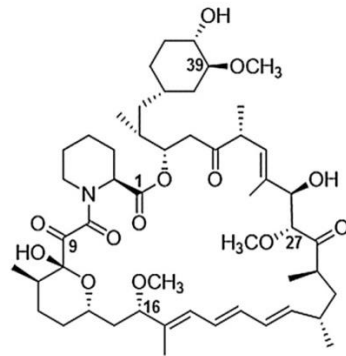


Figure 2: Structure of rapamycin (Taken from Yoo et al., 2017)

Tors are large proteins; the size of Tor1 is 281 kDa (2470 amino acids) and the size of Tor2 is 282 kDa (2474 amino acids). The amino acid sequence of Tor1 is 67 % identical to Tor2 and both are phosphoinositide 3-kinase (PI3K) homologues. Furthermore, Tor1-Tor2 and Tor2-Tor1 hybrids indicated that these kinase domains are interchangeable (Helliwell et al., 1994). They also share a similar domain structure, which is schematically shown in Figure 3: The N-terminal region is characterized by multiple HEAT repeats. A single HEAT repeat forms a pair of interacting antiparallel α -helices. The FAT- and the FATC-domains, which are specific for PIKK families, flank the FRB- and kinase domains in the C-terminal region (Loewith and Hall, 2011). The FRB domain is located N-terminal to the catalytic relevant domain and contains an important serine residue (Ser1972 in Tor1 and Ser1975 in Tor2). Amino acid exchanges (to arginine and isoleucine, respectively) at this site provide rapamycin resistance by preventing interaction with FKBP-rapamycin (Helliwell et al., 1994; Lorenz and Heitman, 1995).

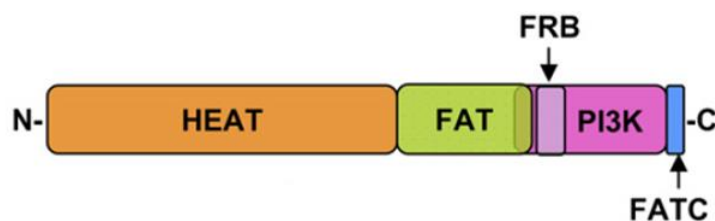


Figure 3: Domain organisation of Tor. The HEAT- (1-2025), FAT- (1319-1919), FRB- (1955-2049), kinase- (2027-2394) and FATC (2395-2470) domains are found in both Tor1 and Tor2. The phosphoinositide 3-kinase (PI3K) homologous domain of the Tor proteins is shown in pink (1802-2394). The amino acid positions of the domains refer to Tor1, which consists of 2470 amino acids in total (taken from Adami et al., 2007).

Tor1 and Tor2 are highly homologous in both structure and function. But how do they differ and why does *S. cerevisiae* need two Tor paralogues?

Unlike Tor2, Tor1 is not essential for vegetative growth. Disruption of *TOR1* leads to a slow growth phenotype whereas disruption of *TOR2* is lethal, but does not cause a cell cycle arrest (Helliwell et al., 1994). It has been shown that Tor2, in addition to its role in the G1 cell cycle, has another function that is essential and cannot be inhibited by FKBP-rapamycin (Zheng et al., 1995). This was later clarified by Loewith et al. They were able to show that Tor2 – but not Tor1 – is also part of another protein complex called TORC2. In contrast to TORC1, FKBP-rapamycin fails to bind to TORC2 and therefore TORC2 disruption does not mimic rapamycin treatment. The reason for this is the presence of the TORC2-unique protein Avo3, which binds adjacent to the FRB domain and thus prevents FKBP-rapamycin binding. This concludes that TORC2 mediates a rapamycin-insensitive Tor2-unique pathway (Karuppasamy et al., 2017; Loewith et al., 2002).

1.3 TORC1 influences ribosomal biogenesis

TORC1 is regulated by environmental influences. Thus, nutrient starvation leads to much the same effects on yeast physiology as exposure to rapamycin. In addition, other noxious stressors like a high salt concentration, redox stress or caffeine also have a negative impact on TORC1 activity. TORC1 itself controls cell growth by regulating a number of cellular processes. Among them, the inhibition of autophagy and stress response programs are prominent examples. More interesting for this study is that TORC1 inactivation leads to the downregulation of transcription and ribosome biogenesis (reviewed in more detail in Loewith and Hall, 2011). A simplified overview of important up- and downstream pathways of TORC1 is shown in Figure 4.

Because TORC2 is primarily involved in cell cycle-dependent polarization of actin cytoskeleton, in sphingolipid biosynthesis and in endocytosis (Loewith and Hall, 2011), this study focuses on the Target Of Rapamycin Complex 1 (TORC1).

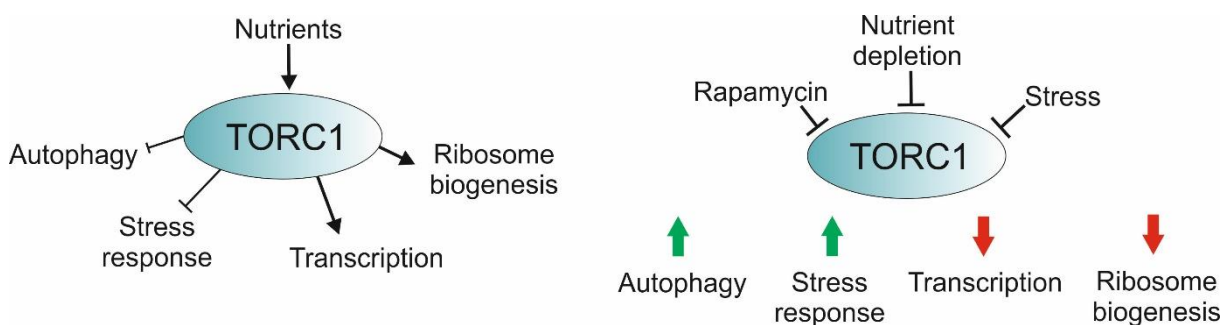


Figure 4: The Target Of Rapamycin Complex 1 (TORC1) processes numerous signals and controls diverse cellular processes. TORC1 is activated by nutrients (left) and inhibited by stress and rapamycin (right). Among other processes, the complex controls cell growth via regulation of autophagy, stress response, transcription and ribosome biogenesis.

Ribosomal biogenesis in *S. cerevisiae* is regulated by TORC1 mainly by transcription of rDNA, RP (Ribosomal Protein) and RiBi (Ribosome Biogenesis) regulons as well as at post-transcriptional level (reviewed in de la Cruz et al., 2018; Loewith and Hall, 2011). The following paragraphs provide more detailed insight into cellular mechanisms used by TORC1 to influence ribosome maturation. A corresponding representation is shown in Figure 5.

The first evidence that rapamycin has an influence on transcription by RNA polymerase I was published in the late 1990s by Zaragoza et al. and Powers and Walter. Both studies showed that rapamycin treatment resulted in a drop in 35S rRNA production (Powers and Walter, 1999; Zaragoza et al., 1998). A few years later, publications followed that gave more detailed insight into the effects of rapamycin on RNA polymerase I (Claypool et al., 2004; Philippi et al., 2010). Specifically, TORC1 inactivation leads to degradation of Rrn3, which is one of the transcription factors of the RNA polymerase I. This correlates with the loss of initiation competent RNAPI-Rrn3 complexes and with the decrease of RNAPI recruitment to the rRNA genes. Consequently, the transcription of the 35S rRNA is downregulated. In starved yeast cells, it has recently been shown that the RNA polymerase I is inactivated through homodimerization and that this is important for the complete clearance of the RNAPI-Rrn3 complexes (Torreira et al., 2017). However, the downregulation of transcription upon TORC1 inactivation cannot entirely be explained by the loss of RNAPI-Rrn3 complexes, suggesting the existence of additional regulatory mechanisms (Philippi et al., 2010; Torreira et al., 2017).

Zaragoza et al. also showed that the amounts of 5S rRNA decreases after rapamycin treatment (Zaragoza et al., 1998). This is because active TORC1 regulates the phosphorylation of the phosphoprotein Maf1. Maf1 is a negative regulator of RNA polymerase III-dependent transcription, which directly binds the polymerase when dephosphorylated. The subsequent rearrangement of RNAPIII subunits interferes with its recruitment to its promoter; and therefore, RNA polymerase III transcription is downregulated (Oficjalska-Pham et al., 2006; Vannini et al., 2010; Wei and Zheng, 2009; Wei et al., 2009).

Furthermore, data regarding TORC1 localisation confirm its role in the regulation of rDNA transcription. Li et al. reported that in normal growing *S. cerevisiae* cells, the kinase Tor1 is found in both cytoplasm and the nucleus. Further investigations showed that TORC1 components (but not TORC2-specific proteins) are associated with 35S promoter and 5S rDNA chromatin, and that the binding takes place in a nutrient-dependent and rapamycin-sensitive manner (Li et al., 2006; Wei et al., 2009).

However, Reiter et al. have shown that the reduction of newly synthesized ribosomal subunits upon TORC1 inactivation precedes the downregulation of RNA polymerase I-dependent transcription. In-

stead, the decrease in r-protein production is the short-term effect of rapamycin treatment, which correlates with the synthesis defect of ribosome subunits. Therefore, the disruption of certain r-proteins as well as rapamycin treatment leads to the nucleolar entrapment of pre-ribosomal Nog1- and Rrp12-particles (Reiter et al., 2011).

TORC1 affects the synthesis of r-proteins and ribosome assembly factors via their regulons and via their translation. The regulation of RP and RiBi regulons occurs using different TORC1 signalling branches. For example, two prominent substrates of TORC1 are the kinase Sch9 and the split zinc-finger protein Sfp1. Both act downstream of TORC1, but have different effects on both RP and RiBi regulons. While Sfp1 is a general transcription activator (de la Cruz et al., 2018; Loewith and Hall, 2011), Sch9 inhibitory phosphorylates the transcription repressors Dot6, Stb3 and Tod6, which are responsible for the recruitment of the RPD3L histone acetyltransferase complex (Huber et al., 2011). Additionally, Sch9 is involved in the nucleus-to-cytoplasm transport of the RNA polymerase III inhibitor Maf1 (Wei and Zheng, 2009). The above-described TORC1-dependent inhibition of the RNAPIII transcription also leads to the decrease of tRNA, which coincides with translational repression (Zaragoza et al., 1998). Furthermore, it was shown that TORC1 is also involved in the regulation of translation initiation (Barbet et al., 1996; Berset et al., 1998; Cherkasova and Hinnebusch, 2003).

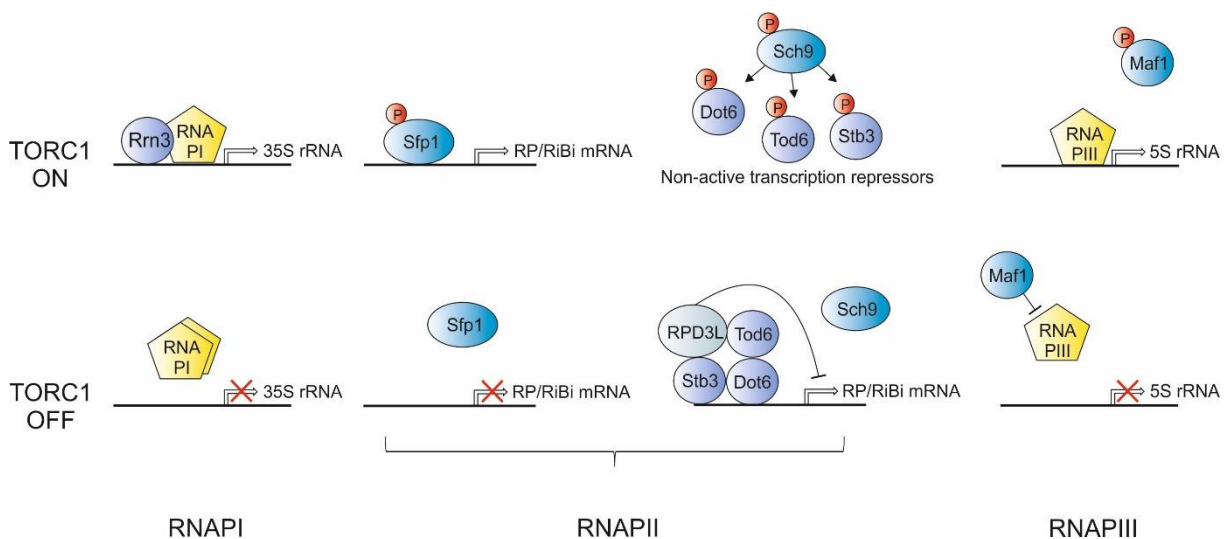


Figure 5: TORC1 regulates the transcription of all three RNA polymerases (RNAPI/II/III). Upon TORC1 inactivation, the synthesis of rRNA and the transcription of RP (Ribosomal Protein) and RiBi (Ribosome Biogenesis) regulons are downregulated. The decrease of pre-rRNA, ribosomal proteins and assembly factors leads to defects in ribosome maturation.

Recently, it has been shown that TORC1 even has an impact on rRNA processing. Kos-Brown et al. have described an alternative pre-rRNA processing pathway using exclusively the A₃ instead of the standard A₂ cleavage site (Figure 6). This pathway results in the production of 23S and 27SA₂ rRNA (the latter is further processed to 27SB rRNA). Total RNA samples showed an accumulation of 35S and 23S rRNA; and tritium-uracil-pulse chase experiments indicated that the alternative pathway is non-productive. A₃ cleavage occurs in cells exposed to heat shock, oxidative stress or rapamycin, and

in post-diauxic cultures. Since resistant *tor1*^{S1972R} strains failed to shift to the alternative pathway after rapamycin treatment, it was concluded that the A₂ to A₃ switch is TORC1 specific. Kos-Braun et al. have also shown that the TORC1 signalling branch, that regulates the switch between the A₂ and A₃ cleavage site, involves the casein kinase 2 (CK2) (Kos-Braun et al., 2017).

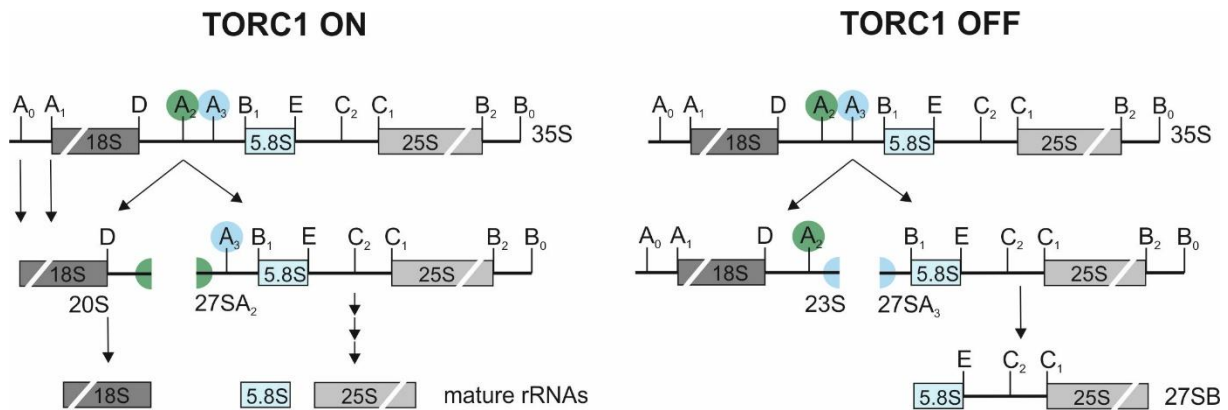


Figure 6: The 35S primary transcript is processed differently upon TORC1 inactivation. Left: In normal growing *S. cerevisiae* cells, pre-rRNA cleavage occurs at the A₀, A₁ and A₂ sites. Right: The 35S pre-rRNA of cells exposed to low nutrients or stress is cleaved at the A₃ site. This represents an alternative, non-productive pre-rRNA processing pathway, which is controlled by TORC1 and CK2.

But this alternative processing pathway is not the only example of post-transcriptional regulation by TORC1 in ribosome maturation. Honma et al. have reported that the complex is involved in the nucleolus to nucleoplasm transfer of 60S precursor particles. In the presence of rapamycin, certain ribosomal assembly factors are enriched in the nucleolus. Their displacement can cause effects in the ongoing ribosomal maturation. One example is the GTP-binding protein Nog1, which is necessary for 60S ribosome biogenesis in both nucleolus and nucleoplasm. Its nucleolar entrapment upon nutrient depletion or rapamycin treatment suggests that TORC1 also regulates later stages of ribosomal biogenesis (Honma et al., 2006). In addition to Nog1, the exposure to rapamycin leads to the nucleolar enrichment of further ribosomal assembly factors like Dim2, Nog2, Nop7, Rlp24 and Rrp12 (Honma et al., 2006; Reiter et al., 2011; Vanrobays et al., 2008). Others, such as the 90S assembly factors Nop1, Nop56 and Nop58, diffuse into the nucleoplasm (Kakihara et al., 2014).

1.4 Role of the early assembly factors Nop58 and Noc2 in TORC1 pathway and in ribosomal biogenesis

As described above, TORC1 has a great effect on ribosome biogenesis. However, further research is required to obtain a more detailed insight into its impact on the composition of pre-ribosomal parti-

cles. For this purpose, Nop58- and Noc2-particles were isolated using tandem affinity purification (TAP) (Puig et al., 2001). It has already been shown that both assembly factors are associated with the TORC1 pathway. As described before, Nop58 diffuses from the nucleolus into the nucleoplasm upon TORC1 inactivation (Kakihara et al., 2014). Noc2, on the other hand, contains an amino acid site (S70), which is more phosphorylated following rapamycin treatment (dissertation of Cremonesi, 2002).

In the ribosome maturation pathway, Nop58 is part of the box C/D small nucleolar ribonucleoproteins (snoRNPs). Box C/D snoRNPs, which are primarily involved in the 2'-O methylation of rRNAs, consist of the core proteins Nop1, Nop56, Nop58 and Snu13, and a box C/D snoRNA (Lafontaine and Tollervey, 1999, 2000; Schimmang et al., 1989; Watkins et al., 2000; Wu et al., 1998). The R2TP protein complex acts as a snoRNP assembly factor in the nucleus and is responsible for the stabilization of unassembled Nop58. The interaction is mediated by Pih1 (also known as Nop17), one of the four R2TP components. Under rapamycin treatment or in the stationary phase, however, the complex is transferred to the cytoplasm. As a consequence, the box C/D snoRNP assembly is impaired (Kakihara et al., 2014).

One prominent box C/D family snoRNA is U3, which base-pairs with nucleotides in the 5'ETS and the pre-18S rRNA. Unlike others of its class, the U3 snoRNP does not act via 2'-O methylation. Much more, it acts as an RNA chaperone complex that stabilizes rRNA elements within the SSU processome and is necessary for co-transcriptional cleavage at sites A₀-A₂ (Klinge and Woolford, 2019).

Noc2 acts like Nop58 in early ribosome maturation, but has a different function. It is involved in the processing of pre-25S and pre-5.8S rRNA, as well as in the intranuclear transport of the 60S pre-ribosomes. It has been shown by immunoelectron and fluorescence microscopy that Noc2 is localised in both nucleolus (60 %) and the nucleoplasm (40 %). Furthermore, Noc2 is found in two distinct complexes (Milkereit et al., 2001). It is recruited co-transcriptionally to the nascent pre-rRNA transcript and interacts there with Noc1 and Rrp5 (Hierlmeier et al., 2013). This module is associated with both 90S and 60S pre-ribosomal particles. Noc2 also can be isolated in a complex with Noc3, which is only associated with 66S pre-ribosomes (Milkereit et al., 2001). It has been suggested that Noc1 is replaced by Noc3 after transport into the nucleoplasm (Milkereit et al., 2001; Nissan et al., 2002).

Considering their function and localisation in the nucleolus and nucleus, respectively (Kakihara et al., 2014; Milkereit et al., 2001), an illustration of Nop58 and Noc2 arrival and release was created (Figure 7).

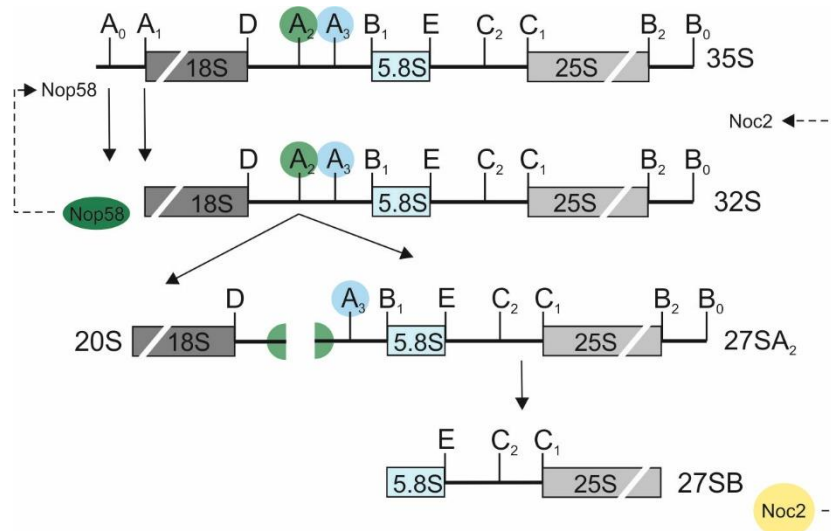


Figure 7: Arrival and release of the nucleolar assembly factors Nop58 and Noc2. Nop58 and Noc2 are recruited co-transcriptionally to the primary 35S transcript. Considering its function and nucleolar and nucleoplasmic localisation, Noc2 remains associated with the 66S pre-ribosomal particle until formation of 27SB rRNA. If it is part of the U3 snoRNP, Nop58 dissociates prior to the formation of the 43S-particle. Finally, both proteins are released and recycled to the 35S primary transcript. It should be noted that the actual release of the two assembly factors has not yet been determined. Furthermore, Nop58 is also part of other box C/D snoRNPs and can therefore be associated with further rRNA intermediates.

The goal of this study was to determine the protein and rRNA content of early ribosomal particles before and after rapamycin treatment to gain better insights into the role of the TORC1 complex in ribosome biogenesis. Further conclusions should be drawn by examining *tor1* mutants. Additionally, a possible effect on ribosome biogenesis of these mutations should be investigated by comparison with samples of the respective untreated *TOR1* wild-type strain.

2 Material and Methods

2.1 *Saccharomyces cerevisiae* strains and media

Saccharomyces cerevisiae strains used in this study are summarized in Table 1. The strains were grown in Yeast Extract Peptone Dextrose (YPD) medium. Synthetic Dextrose Complete (SDC) medium supplemented with all amino acids was only used for fluorescence microscopy (see 2.6). The media composition is described in Table 2. Culture plates were made by adding 2 % agar. For selective growth (see 2.2.2), geneticin disulphate (Carl Roth) in a final concentration of 300 µg/ml was added to YPD after sterilisation and cooling the media to about 60 °C.

Table 1: *Saccharomyces cerevisiae* strains used in this study

Collection #	<i>S. cerevisiae</i> strain	Genotype	Source
6008	W303_Rlp7-YFP	<i>MATa, leu2, ura3, his3, ade2, trp, RLP7-YFP</i>	Christina Morgenstern
6393	LMA158	<i>MATa, trp1-289, ura3-52, ade2, leu2-3,112, Arg4(RV-), Nog1-TAP::TRP1</i>	Micheline Fromont-Racin, Institute Pasteur
6584A	Nsa1-TAP	<i>MATa, ura3, trp1, his3, leu2, NSA1-TAP::kITRP1</i>	Dieter Kressler, University of Freiburg
6589D	Nop4-GFP_Hho1-mCherry	<i>MATa, leu2, ura3, his3, meth15, NOP4-GFP::HIS3, Hho1-mCherry::hphNT1</i>	Christina Mauerhofer
6590C	Nsa1-GFP_Hho1-mCherry	<i>MATa, leu2, ura3, his3, meth15, NSA1-GFP(HIS3), Hho1-mCherry::hphNT1</i>	Christina Mauerhofer
6591C	Nog1-GFP_Nop58-mCherry	<i>MATa, leu2, ura3, his3, meth15, NOG1-GFP::HIS3, NOP58-mCherry::hphNT1</i>	Christina Mauerhofer
6594D	Noc2-GFP_Nop58-mCherry	<i>MATa, leu, ura3, his3, meth15, NOC2-GFP::HIS3, NOP58-mCherry::hphNT1</i>	Christina Mauerhofer
6613C	HHY110/Noc2-TAP	<i>MATa, leu2, ura3, his3, ade2, tor1-1, fpr1::NAT, PMA1-2xFKBP12::TRP1, NOC2-TAP::HIS</i>	Manuela Grassegger

Collection #	<i>S. cerevisiae</i> strain	Genotype	Source
6616B	Nop58-TAP/Utp20-HA/Utp14-Flag	<i>MATα, ade2, arg4, leu2, ura3, trp1, NOP58-TAP::TRP, UTP20-HA::KanMX, UTP14-Flag::natNT2</i>	Gertrude Zisser
6616C	Noc2-TAP/Utp20-HA/Utp14-Flag	<i>MATα, ade2, arg4, leu2, ura3, trp1, NOC2-TAP::TRP, UTP20-HA::KanMX, UTP14-Flag::natNT2</i>	Gertrude Zisser
6673B	TS161	<i>MATα, ura3-52</i>	Tatsuya Maeda, University of Tokyo
6673C	TS184	<i>MATα, ura3-52, tor1^{L2134M}</i>	Tatsuya Maeda, University of Tokyo
6678B	TS161_Noc2-TAP	See TS161; <i>NOC2-TAP::KanMX</i>	This study
6678D	TS184_Noc2-TAP	See TS184; <i>NOC2-TAP::KanMX</i>	This study

Table 2: Yeast Media recipes used in this study. All media were sterilized for at least 25 minutes at 121 °C either in an autoclave or in a CertoClav. For the SDC media, solution A and solution B were sterilized separately in a CertoClav.

Medium	Component	Concentration	pH
YPD	Bacto™ Yeast Extract, Technical (Becton Dickinson)	10 g/l	5.5
	Bacto™ Peptone (Becton Dickinson)	20 g/l	
	D(+)-Glucose 1-hydrate (PanReac AppliChem)	20 g/l	
	European Agar (Becton Dickinson) – optional	20 g/l	
	<u>Solution A</u>		5.5
SDC	Yeast Nitrogen Base w/o Amino Acids and Ammonium Sulphate (Becton Dickinson)	1.40 g/l	
	Ammonium sulphate (SERVA)	5 g/l	
	CSM Complete Supplement Mixture (MP Biomedicals)	0.79 g/l	
	Adenine (SERVA)	0.05 g/l	
	<u>Solution B</u>		
	D(+)-Glucose 1-hydrate (PanReac AppliChem)	20 g/l	

The pH values of media, buffers and solutions were adjusted with 1 N sodium hydroxide solution (Carl Roth), 1 N potassium hydroxide solution (Carl Roth) or 1 N/32 % hydrochloric acid (Carl Roth), depending on the initial pH value and content.

2.2 TAP tagging of *NOC2*

TAP tagged strains were needed to isolate whole pre-ribosomal complexes using an adapted version of the tandem affinity purification (*TAP*) procedure (Puig et al., 2001) (see 2.3). *TAP* tagging of *NOC2* in strains TS161 and TS184 (Table 1) was performed by homologous recombination of *TAP-KanMX* cassettes by linear transformation according to the lithium-acetate method (Ito et al., 1983). After growth on selective media, the cell colonies were controlled for correct *TAP* tag integration by colony-PCR and western blot analysis. All other *TAP*-tagged strains (Table 1) were taken from the house's own strain collection. Primers used during this procedure are listed in Table 3.

Table 3: Primers used in this study

Primer name	Sequence	Description
Noc2_F2	ATTAAACAGTCTGGAAAGTGATGATGACAACGAAGATGTT	Tagging cassette
	GAAATGTCAGACGCTcggATCCCCGGGTTAATTAA	amplification
Noc2_rev	CATTATAGACTTAACTATTGAATTCAAGACAAAAAATCAA	Tagging cassette
	ATCTTGCTGAGTTGgaaTTCGAGCTCGTTTAAAC	amplification
KanR5'b	CAAGACTGTCAAGGAGGG	Control primer
Noc2_control_primer	CTTAACAAACGTTTATCAACTG	Control primer

2.2.1 Amplification of the *TAP-KanMX* tagging cassette

Amplification of the *TAP-KanMX* cassette was performed by polymerase chain reaction (PCR). The plasmid pFA6a *TAP-KanMX* (Brigitte Pertschy's tagging plasmid collection #3039; originally from University of Heidelberg) was used as a template. Primers containing F2/S2 linkers were *NOC2* specific. PCR reaction setup and thermocycling conditions are shown in Table 4 and 5.

350 μ L of pooled PCR products were frozen and then centrifuged in the presence of vacuum using a lyophilisation system with Edwards vacuum pump. The volume was reduced to about 50 μ L. Until used for linear transformation, the construct was stored at -20 °C.

Table 4: PCR reaction setup for *TAP-KanMX* tagging cassette amplification. All reaction components were assembled on ice. Phusion polymerase was added at the end. For negative control, the template was replaced by Aqua bidest. "Fresenius".

Component	50 μ l reaction
5x Phusion HF Buffer (Thermo Fisher Scientific)	10 μ l
dNTPs [2 mM dATP/dCTP/dGTP/dTTP] (Thermo Fisher Scientific)	5 μ l
Forward primer: Noc2_F2 [10 μ M]	5 μ l
Reverse primer: Noc2_rev [10 μ M]	5 μ l
Template: #3039 pFA6a TAP-KanMX [200 ng/ μ l]	0.50 μ l
DMSO (Thermo Fisher Scientific)	0.50 μ l
Phusion polymerase [2 U/ μ l] (Thermo Fisher Scientific)	0.50 μ l
Aqua bidest. "Fresenius" (Fresenius Kabi)	to 50 μ l

Table 5: Thermocycling conditions for *TAP-KanMX* tagging cassette amplification

Step	Temperature	Time	Cycles
Initial denaturation	98 °C	30 seconds	1
Denaturation	98 °C	15 seconds	
Annealing	55 °C	1 minute	35
Amplification	72 °C	2 minutes	
Final Extension	72 °C	7 minutes	1
Hold	4 °C	∞	

2.2.2 Linear transformation

TS161 and TS184 cell cultures were grown in 50 ml YPD and harvested by centrifugation (5-10 minutes, 3500 rpm, room temperature) after an OD₆₀₀ value of 0.5 was reached. The pellets were then resuspended in 10 ml sterile lithium acetate solution (Table 6) and centrifuged under the same conditions. This procedure was repeated. After resuspension in 300 μ l sterile lithium acetate solution, the cells were incubated for 30 minutes at 30 °C in a water bath. After this incubation step, two transformation attempts per culture were assembled: Both contained 300 μ l PEG solution (Table 6), 50 μ l lithium acetate-treated cells and 15 μ l herring sperm. One of the attempts was mixed with 10 μ l of the concentrated PCR product containing *TAP-KanMX* tagging cassettes; and the other attempt served as a negative control. After 30 seconds of shaking in the vortex-mixer, the cells in the mixtures were regenerated for 30 minutes in a 30 °C water bath and then heat shocked for 20 minutes in a 42 °C water bath. Cells were then collected by gentle centrifugation (2 minutes, 3000 rpm, room temperature) and resuspended in 10 ml YPD. After 5 hours of regeneration (30 °C, 170 rpm), the cells

were collected again and YPD was discarded. The remaining cell suspensions were divided and plated on selective plates (YPD supplemented with geneticin).

Table 6: Solutions used for linear transformation. The solutions were freshly prepared and sterile filtered using sterile PVDF Rotilabo®-syringe filters (pore size 0.45 µm, Ø outer 33 mm, Carl Roth).

Solution	Component	Concentration
Lithium acetate solution	Lithium acetate dihydrate (Sigma-Aldrich)	0.1 M
	Tris-HCl, pH 7.5 (TRIS PUFFERAN® by Carl Roth)	10 mM
	Ethylenediamine tetraacetic acid disodium salt dihydrate/EDTA (Carl Roth), pH 8	1 mM
PEG solution	Lithium acetate (Sigma-Aldrich)	10.20 g/l
	Tris-HCl, pH 7.5 (TRIS PUFFERAN® by Carl Roth)	10 mM
	EDTA (Carl Roth), pH 8	1 mM
	Polyethylene glycol 400 (Carl Roth)	400 g/l

2.2.3 Colony-PCR and agarose gel electrophoresis for *TAP* tag control

Colonies that had grown on YPD supplemented with geneticin were further examined for the correct positioning of the *TAP* tag. Colony-PCR was carried out for this purpose. The colonies to be tested were spread on new culture plates the evening before. From these plates, fresh cell material was resuspended in 20 µl Aqua bidest. “Fresenius” and incubated at 95 °C for 10 minutes. 7.5 µl supernatant of the suspension were used as a template after short centrifugation (1 minute, full speed). PCR reaction setup and thermocycling conditions are show in Table 7 and 8.

Table 7: Colony-PCR reaction setup for *TAP* tag control. All reaction components were assembled on ice. Taq polymerase was added at the end.

Component	25 µl reaction
Template DNA	7.50 µl
10x ThermoPol Reaction buffer (New England Biolabs)	2.50 µl
dNTPs [2 mM dATP/dCTP/dGTP/dTTP] (Thermo Fisher Scientific)	2 µl
Forward primer: Noc2_control_primer [10 µM]	1 µl
Reverse primer: KanR5'b [10 µM]	1 µl
Taq polymerase [5 U/µl] (New England Biolabs)	0.50 µl
Aqua bidest. “Fresenius” (Fresenius Kabi)	to 25 µl

Table 8: Thermocycling conditions for colony-PCR

Step	Temperature	Time	Cycles
Initial denaturation	95 °C	5 minutes	1
Denaturation	95 °C	1 minute	
Annealing	55 °C	1 minute	35
Amplification	72 °C	2 minutes	
Final Extension	72 °C	7 minutes	1
Hold	4 °C	∞	

After PCR amplification, 2 µl of the products were mixed with 6x DNA Loading Dye (Thermo Fisher Scientific) to a final concentration of 1x. Samples were then separated through a 1 % agarose gel [1 g agarose, universal (VWR International) dissolved in 100 ml 1xTAE buffer containing ethidium bromide (Carl Roth)] at 100 V. 0.5xTAE was used as running buffer and 0.5 µg λ DNA/*EcoRI*+*HindIII* (Thermo Fisher Scientific) as a size control marker. 50xTAE buffer recipe is listed in Table 9.

Table 9: Components of the 50xTAE buffer used for gel electrophoresis

Component	1 litre
TRIS PUFFERAN® (Carl Roth)	242 g
Glacial acetic acid (Carl Roth)	57.1 mL
EDTA (Carl Roth), pH 8	100 ml
Distilled water	to 1 litre

2.2.4 “Quick ‘n’dirty” yeast protein extraction

In order to control *TAP* tag expression of positive transformants, a western blot analysis was also performed. This involved protein extraction after chemical cell lysis.

Two OD₆₀₀ units of each overnight culture (culture conditions: 30 °C, 170 rpm) were harvested in a table centrifuge (1 minute, full speed) and were resuspended in 200 µl of a 2-mercaptoethanol solution (Table 10). After 10 minutes of incubation on ice, 200 µl of a 50 % trichloroacetic acid (TCA, ≥99 % from Carl Roth) solution was added to precipitate the proteins. The mixture was then stored on ice for 10 minutes again. After 10 minutes of centrifugation (13000 rpm, 4 °C) the supernatant was discarded. To remove TCA residues, the pellet was washed with 1 ml cold sterile water by a further centrifugation step (same conditions). The supernatant was discarded again and the pellet was resuspended in 100 µl 2x final sample buffer (FSB; Table 14). The protein samples were stored at -20 °C until use.

To confirm the expression of the *TAP* tag in later western blot analysis, proteins were also extracted from a negative (strain TS161, see Table 1) and from a positive control (strain Noc2-TAP/Utp20-HA/Utp14-Flag, see Table 1).

Table 10: 2-Mercaptoethanol solution used for yeast protein extraction

Component	Concentration
2-Mercaptoethanol (Carl Roth)	7.5 %
Sodium hydroxide (Carl Roth)	1.85 M
TRIS PUFFERAN® (Carl Roth)	10 mM

2.2.5 Control of *TAP* tag expression using western blot analysis

Protein samples dissolved in 2xFSB buffer were denatured for 10 minutes at 95 °C and centrifuged at 13000 rpm for at least 3 minutes. 10 µl of these samples and 3 ml of the size control marker PageRuler Prestained Protein Ladder (10 to 180 kDa; Thermo Fisher Scientific) were separated by sodium dodecyl sulphate polyacrylamide gel electrophoresis (SDS-PAGE) at 16 mA. This was performed using tris-glycine running buffer (Table 11), a homemade 12.5 % polyacrylamide gel and the equipment from Hoefer (Mighty Small Basic Unit, 8x7 cm). Blotting and antibody detection (using α-CBP, see Table 13) was performed as described in chapter 2.4.3 and 2.4.4. Since the homemade gel was thinner than the bought one, blotting was done for only 1 hour.

Table 11: Tris-glycine running buffer used for SDS-PAGE with 12.5 % polyacrylamide gel

Component	Concentration
TRIS PUFFERAN® (Carl Roth)	0.25 M
Glycerol (VWR International)	1.90 M
SDS (Carl Roth)	1 %

2.3 Tandem affinity purification (TAP)

2.3.1 Growth condition and cell harvest

Two litres of YPD (in 5-litre baffled flasks) were inoculated with a pre-culture to an OD₆₀₀ of about 0.0003 to 0.01 (depending on the growth rate of the culture), incubated at 30 °C and agitated at 110 rpm. These cultures were grown to an OD₆₀₀ of 1.0 to 1.3 and then treated either with rapamycin (LC Laboratories) in a final concentration of 3 µg/ml or with the drug vehicle (0.10 % DMSO; Carl Roth) alone. After 2, 15 or 30 minutes of treatment, the cell cultures were harvested by centrifuga-

tion (5000 rpm, 4 °C, 3 minutes minimum). Cell pellets were resuspended in 20 ml of distilled sterile water supplemented with 3 µg/ml rapamycin or with the adequate amount of DMSO. After a washing step (centrifugation at the same conditions), the cell pellets were stored in 50 ml Sarstedt tubes at -20 °C.

2.3.2 Cell lysis

The pellets were defrosted on ice and resuspended with the same volume of lysis buffer (Table 12), including 0.5 mM phenylmethanesulfonyl fluoride [PMSF (Sigma-Aldrich) dissolved in 2-Propanol (Carl Roth)], 1 mM dithiothreitol/DTT (Carl Roth) and Protease-Inhibitor Mix FY (SERVA; used according to the manufacturer's instructions). Cell disintegration was performed with 1.5-fold volume glass beads (0.40-0.60 mm; Sartorius), relative to the pellet volume in a Merckenschlager disintegrator (B. Braun), for 4 minutes under CO₂-cooling. The glass beads and cell debris were then removed by several centrifugation steps at 4 °C, whereby the supernatants were transferred into a fresh centrifugation tube after each step: The first centrifugation step was carried out for 10 minutes at 5000 rpm, the second for 10 minutes at 18500 rpm and the last for at least 30 minutes at 18500 rpm. The supernatant after the last centrifugation step is called crude extract (CE). Aliquots of CE were taken for later northern blot and SDS-PAGE analyses.

2.3.3 Purification

Prior to their usage in purification, IgG Sepharose™ beads (GE Healthcare) and 1 µm BcMag™ Epoxy-Activated magnetic beads (Bioclone) conjugated with rabbit IgG (Dunn Labortechnik) were washed three times with lysis buffer.

The CE was then incubated under constant rotation for 90 minutes at 4 °C either with 150 µl IgG beads or with 200 µl magnetic beads. After this binding step, the beads were washed two times with lysis buffer (including 1 mM DTT) and one time with cleavage buffer (Table 12) (including 0.5 mM DTT) to eliminate unspecific binding. In between, the buffer was removed by a gentle centrifugation step (3 minutes, 3000 rpm, 4 °C) when IgG beads were used, or by a magnet separator when magnetic beads were used. TEV protease cleavage was done by adding 2.5 µl or 4 µl TEV protease (home-made; diluted in cleavage buffer with 0.5 mM DTT) to the IgG beads or to the magnetic beads, respectively, and by incubation under constant rotation at room temperature for 60 minutes. 1 µl RiboLock RNase inhibitor (40 U/µl; Thermo Fisher Scientific) was added per sample to preserve the RNA during TEV cleavage. After this incubation step, the ribosomal particles of interest were dissolved in the supernatant. This supernatant is called TEV eluate and was collected. While the elution of the magnetic bead samples was done using a magnetic separator, the elution of the IgG bead samples was done using Mobicol "Classic" M1002 (MoBiTec) columns. The beads were then discard-

ed. 15 µl of each TEV eluate sample was taken and stored at -70 °C for later northern blot analyses. The remaining residues of the TEV eluate samples were collected at -20 °C for later western blot analyses.

Table 12: Buffers used for tandem affinity purification

Buffer	Component	Concentration
Lysis buffer, pH 7.5	N-(2-hydroxyethyl)piperazine-N'-2-ethane sulfonic acid/HEPES (SERVA)	20 mM
	Potassium chloride (Fluka)	10 mM
	Magnesium chloride hexahydrate (Carl Roth)	2.50 mM
	EGTA (Carl Roth)	1 mM
Cleavage buffer, pH ~7.5	HEPES (SERVA)	20 mM
	Potassium chloride (Fluka)	10 mM
	Magnesium chloride hexahydrate (Carl Roth)	2.50 mM
	EGTA (Carl Roth)	1 mM
	Sodium chloride (Carl Roth)	100 mM

2.4 Western blot analysis of TEV eluates

2.4.1 SDS-PAGE

TEV eluate samples (for growth conditions and purification see 2.3) were mixed with 5xFSB (Table 14) to get a final concentration of 2xFSB. Before loading the gel, the samples were denatured for 10 minutes at 95 °C and centrifuged (full speed) for at least 3 minutes. In order to estimate protein sizes, 3 µl of PageRuler Prestained Protein Ladder (10 to 180 kDa; Thermo Fisher Scientific) were also loaded onto the gel. NuPAGE™ 4-12 % Bis-Tris gels (1.0 mmx15 well) and 1x NuPAGE® MOPS SDS Running Buffer (Life Technologies) were used both for colloidal blue staining as well as for blotting. The samples loaded on the gel were separated in an XCell SureLock™ Electrophoresis Cell (Life Technologies) at 100 V.

2.4.2 Colloidal blue staining

Stainer A and B of the Novex® Colloidal Blue Staining Kit (Invitrogen) were used to make protein bands present in SDS gels visible. For staining, the SDS gels were first shaken 10 to 20 minutes in a fixer solution (Table 14) and then 10-20 minutes in 11 ml Aqua bidest. "Fresenius" (Fresenius Kabi), 4 ml methanol (Carl Roth) and 4 mL Novex® Stainer A. After adding 1 ml Novex® Stainer B, the gels

were incubated overnight in the shaker. The next day the gels were washed at least three times for 10 minutes with distilled water. All steps were performed at room temperature. The gels were stored in 3 % acetic acid (96 % by Carl Roth) in the fridge. For the loading of a second SDS gel, which was needed for blotting, the colloidal blue-stained gel was used to adapt the amounts of the samples to each other.

2.4.3 Blotting

For blotting, polyvinylidene difluoride membranes (Roti®-PVDF, 0.45 µm; Carl Roth) were activated in methanol (Carl Roth) for at least 1 minute. Within a time-period of 2 hours, the separated proteins were transferred onto the membrane at 220 mA using a tank blot system (Hoefer) filled with CAPS buffer (Table 14). Afterwards the membranes were blocked overnight at 4 °C by shaking in a 0.5 % powdered milk (Carl Roth) solution (dissolved in 1xTST; see Table 14).

2.4.4 Antibody detection

All antibodies used in this study are summarized in Table 13. For incubation, membranes were shaken in a primary and then in a secondary antibody dilution or in a conjugated antibody dilution at room temperature. After each incubation step, the membranes were washed three times for 5 minutes with 1xTST. For detection with the ChemiDoc™ Touch Imaging System (Bio-Rad), they were incubated for 3 minutes with Clarity western luminol/enhancer solution and peroxide solution (Clarity™ Western ECL Substrate by Bio-Rad) in a ratio of 1:1. After each detection step, stripping of antibodies was performed by shaking in stripping buffer (Table 14) for 20 minutes at about 60 °C. For overnight storage, membranes were blocked as described above. For longer storage, membranes were dried and stored at room temperature; then before re-use, they were shaken for at least 30 minutes in 1xTST with a 0.5 % powdered milk solution.

Table 13: Antibodies used in this study. Antibodies used were diluted in 1xTST with 1 % powdered milk. Unless otherwise described, Peroxidase labelled α-rabbit antibody was used as secondary antibody.

Antibody	Dilution	Source
α-CBP	1:5000	Sigma-Aldrich
α-Cic1	1:5000	University of Stuttgart
α-Drg1	1:7500	Zakalskiy et al., 2002
α-Ebp2	1:5000	M. A. McAlear
α-Erb1	1:5000	J. de la Cruz
α-Flag*	1:15000	Sigma-Aldrich
α-HA*	1:5000	Roche

Antibody	Dilution	Source
α -Has1	1:5000	J. de la Cruz
α -Mak11	1:2500	M. Fromont-Racine
α -Nhp2	1:5000	Y. Henry
α -Noc1	1:5000	University of Regensburg
α -Noc2	1:5000	University of Regensburg
α -Noc3	1:5000	University of Regensburg
α -Nog1	1:5000	M. Fromont-Racine
α -Nog2	1:5000	M. Fromont-Racine
α -Nop1	1:30000/1:50000	E. Hurt
α -Nop2**	1:2000	Invitrogen
α -Nsa2	1:5000	M. Fromont-Racine
α -Phosphoserine	1:1000	Provided by K. Preiß-Landl
α -Rcl1	1:5000	A. Henras
α -Rok1	1:5000	K. Karbstein
α -Rpa135	1:3000	M. Oaks
α -Rpl5	1:3000	
α -Rpl16	1:40000	S. Rospert
α -Rrp12	1:5000	M. Dosil
α -Rsa4	1:10000/1:15000	M. Remacha
α -Sof1	1:300/1:900	E. Hurt
α -Tif6	1:5000	GeneTEX
α -Ytm1 (cross-reaction with Nop7)	1:5000	J. de la Cruz
Peroxidase labelled α -rabbit***	1:15000	Sigma-Aldrich
Peroxidase labelled α -mouse***	1:10000	Amersham Biosciences

*Conjugated antibody; no secondary antibody was necessary/**Peroxidase labelled α -mouse antibody was used as secondary antibody/****Secondary antibody

2.4.5 Semi-quantitative analysis of western blot results

First, western blot results were analysed using the software Image Lab (version 5.2 build 14). The band intensity was measured by forming rectangles over detected protein bands using the volume tool "Rectangle". "Adjusted volume" values were transferred and further analysed in a Microsoft Excel file. For each membrane the value of the control *TOR1* wild-type sample was set to 100 %. The percentages of the respective rapamycin-treated or *tor1* mutant samples were determined in rela-

tion according to this. In addition, these calculated values were similarly correlated with the values of their respective bait protein.

Table 14: Buffers and solutions used for western blot analysis

Buffer or solution	Component	Concentration
5x Final sample buffer	Tris-HCl, pH 6.8 (TRIS PUFFERAN® by Carl Roth)	312 mM
	SDS (Carl Roth)	10 %
	DTT (Carl Roth)	600 mM
	87 % Glycerol (VWR International)	43.5 %
	Bromophenol blue sodium salt (Carl Roth)	0.02 %
Fixer solution	Methanol (Carl Roth)	50 %
	Acetic acid (Carl Roth)	10 %
CAPS transfer buffer	CAPS (Carl Roth), pH 11	100 mM
	Methanol (Carl Roth)	10 %
10xTST, pH 7.4	TRIS PUFFERAN® (Carl Roth)	500 mM
	Sodium chloride (Carl Roth)	1.50 M
	Tween20 (Carl Roth)	1 %
Stripping buffer	2-Mercaptoethanol (Carl Roth)	100 mM
	SDS (Carl Roth)	2 %
	Tris-HCl, pH 6.7 (TRIS PUFFERAN® by Carl Roth)	62.50 mM

2.5 Northern blot analysis of CEs and TAP-purified samples

2.5.1 RNA preparation

CE, TEV eluate and magnetic bead samples (for growth conditions and purification see 2.3) were stocked up to 300 µl with Aqua bidest. "Fresenius". This was followed by adding 100 µl 4x lysis buffer (Table 16) and 300 µl phenol:chloroform:isoamyl alcohol in a ratio of 25:24:1 (P-C-I; Carl Roth-Carl Roth-Merck) per sample. These mixtures were shaken for 1 minute in a vortex-mixer and centrifuged at 13000 rpm for 2-5 minutes. The upper phases were removed, mixed with 200 µl P-C-I using a vortex-mixer and centrifuged again. After this, approximately 200 µl chloroform:isoamyl alcohol (24:1) were added to the upper phases to remove phenol residues. After a final mixing and centrifugation step, the upper phases were collected again and precipitated with sodium acetate (1/10 the sample volume) (Table 16), ethanol absolute (2.5 times sample the volume) (Chem-Lab) and 1 µl GlycoBlue™ Coprecipitant (Invitrogen) for at least 20 minutes or overnight at -20 °C. After precipitation, the sam-

ples were centrifuged 15 minutes at 13000 rpm at 4 °C. The supernatants were removed and the pellets were dried and dissolved as follows: CE pellets were mixed with 30 µl Aqua bidest. “Fresenius” and pellets from TAP-purified samples were mixed with 35.5 µl Aqua bidest. “Fresenius” and 11.5 µl 4x RNA loading dye (Table 16). The RNA concentration of the CE samples was determined using a NanoDrop spectrophotometer (Thermo Fisher Scientific). 1 µg RNA of each CE sample was mixed with Aqua bidest. “Fresenius” and 4x RNA loading dye (finally simply concentrated) to an end volume of 46 µl. All diluted RNA samples were divided into two tubes and stored at -20 °C.

2.5.2 RNA gel electrophoresis

The RNA samples were heated at 65 °C for 10 minutes and then centrifuged for 5 minutes at room temperature (13000 rpm). 20 µl of the RNA samples were loaded on the gels and separated at 60 V for approximately 8 hours. The components of the RNA gels are listed in Table 15. MOPS buffer supplemented with formaldehyde was used as running buffer (Table 16).

Table 15: Composition of a single RNA agarose gel (1.5 %) used for RNA gel electrophoresis. Agarose was dissolved in water and 10x MOPS buffer using a microwave. After cooling, formaldehyde and ethidium bromide were added.

Component	Mass or volume
Agarose, universal (VWR International)	4 g
Aqua bidest. “Fresenius” (Fresenius Kabi)	220 ml
10x MOPS buffer (Table 16)	25 ml
37 % Formaldehyde solution (Sigma-Aldrich)	4.50 ml
Ethidium bromide, 10 mg/ml (Carl Roth)	10 µL

2.5.3 Blotting

Within 18 hours minimum, the separated RNA samples were transferred from the RNA agarose gels onto an Amersham Hybond™-N (GE Healthcare) membrane using the capillary-method. The transfer took place at room temperature. 20x SSC buffer (Table 16) and blotting papers (Bio-Rad) were used. After blotting, the membranes were carefully cleaned with Aqua bidest. “Fresenius”. The RNA was then cross-linked to the membranes with ultraviolet radiation (2x 150 MJ/cm²). To visualize RNA on the membranes, the membranes were stained for at least 15 minutes with a methylene blue solution (Table 16). For storage until radioactive hybridization analysis, the membranes were imbedded in autoclave bags and frozen at -20 °C.

2.5.4 Radioactive hybridization analysis

Radioactive hybridization analysis was performed by Lisa Kofler, BSc, MSc and Magdalena Gerhalter, BSc.

Hybridization was done overnight at 42 °C or 37 °C (E-C2 probe) using one of the 5'-³²P-labelled oligonucleotides listed in Table 17. Before detection by autoradiography, the membranes were washed three times at 42 °C for 20 minutes. Afterwards, the membranes were regenerated by washing in 1 % SDS (Carl Roth). The composition of hybridization and washing buffer is listed in Table 16.

Table 16: Buffers and solutions used for northern blot analysis

Buffer or solution	Component	Final Concentration
4x Lysis buffer	Tris-HCl, pH 7.5 (TRIS PUFFERAN® by Carl Roth)	40 mM
	EDTA (Carl Roth), pH 8	40 mM
	SDS (Carl Roth)	2 %
Sodium acetate, pH 5.2	Sodium acetate trihydrate (Carl Roth)	3 M
10x MOPS buffer pH 7	3-(N-morpholino)propanesulfonic acid (Car Roth)	200 mM
	Sodium acetate trihydrate (Carl Roth)	50 mM
	EDTA (Carl Roth)	10 mM
5x RNA loading dye*	Saturated bromophenol solution (bromophenol blue sodium salt by Carl Roth)	0.16 %
	EDTA (Carl Roth), pH 8	4 mM
	37 % Formaldehyde solution, (Sigma-Aldrich)	2.66 %
	87 % Glycerol (VWR International)	20.01 %
	Formamide (Fluka)	30.38 %
1x MOPS running buffer	10x MOPS buffer	40 %
	37% Formaldehyde solution (Sigma-Aldrich)	10 %
20x SSC buffer pH 7	Sodium chloride (Carl Roth)	0,74 %
	tri-Sodium citrate dihydrate (Carl Roth)	3 M
Methylene blue solution	Methylene blue (Loba Chemie)	0.30 M
	Sodium acetate trihydrate (Car Roth), pH 5.2-5.5	0.20 g/l
	di-Sodium hydrogen phosphate dihydrate (Carl Roth), pH 7.2	10 %
Hybridization buffer	EDTA (Carl Roth), pH 8	0.50 M
	SDS (Carl Roth)	1 mM
Washing buffer	di-Sodium hydrogen phosphate dihydrate (Carl Roth), pH 7.2	7 %
	SDS (Carl Roth)	40 mM
		1 %

*More bromophenol was added to enhance the blue colour. For this reason, the RNA loading dye was less concentrated.

Table 17: 5'-³²P-labelled oligonucleotides used for radioactive hybridization analysis

Probe	Sequence
5.8S	5'-GCGTTCTTCATCGATGC-3'
18S	5'-CATGGCTTAATCTTTGAGAC-3'
25S	5'-CTCCGCTTATTGATATGC-3'
A ₂ -A ₃	5'-TGTTACCTCTGGGCCC-3'
D-A ₂	5'-GACTCTCCATCTTGTCTTCTTG-3'
E-C ₂	5'-GGCCAGCAATTTCAAGTTA-3'

2.6 Fluorescence Microscopy

SDC medium with all amino acids and an additional adenine content (see 2.1) was used for the fluorescence microscopy instead of the YPD medium. GFP-, mCherry- and YFP-tagged strains (Table 1) were incubated overnight at 30 °C while being agitated at 170 rpm. When the cultures reached an OD₆₀₀ of 0.6-1.0, they were treated for 15, 30 or 45 minutes either with rapamycin (3 µg/ml) or with the drug vehicle (0.10 % DMSO) alone. After treatment, the cells were spun down in a tabletop centrifuge (13000 rpm, 1 minute) and 2.5 µl were transferred onto a microscopy slide. For fluorescence microscopy, the equipment used was: a narrow band enhanced GFP, mCherry and YFP filter (Zeiss) on a Zeiss Axioskop microscope and the MetaMorph software version 6.2r4 (Universal Imaging).

3 Results

3.1 Effect of Rapamycin on rRNA and protein levels of Nop58-particles

To observe possible changes in the particle composition upon TORC1 inactivation, very early pre-ribosomal particles were isolated after different times of rapamycin treatment using a TAP fusion to the snoRNP component Nop58 as bait protein. This snoRNP co-transcriptionally associates with 35S pre-rRNA and is released shortly after A₂ cleavage from the pre-ribosome (for references see 1.4). Control samples were treated with the drug vehicle dimethyl sulfoxide (DMSO) in the equivalent final concentration. Throughout this study, samples that were exposed only to the drug vehicle are defined as "untreated". The pre-rRNA and protein composition of untreated and treated pre-ribosomal particles were analysed by northern and western blotting. These results from two biological replicates are illustrated in Figure 8 and 9.

The effect of rapamycin on the composition of the Nop58-TAP containing particle was studied after treatment periods between 2 and 30 minutes and revealed that rapamycin indeed influences the protein composition of the pre-ribosome (Figure 8). The effect was particularly pronounced after 30 minutes of drug treatment. With the exception of Nop1 and Rpa135, protein levels decreased noticeably for all investigated proteins. Rpa135 levels did not change and Nop1 levels seemed to accumulate. Because Nop1 and Nop58 are box C/D snoRNP core proteins, it is likely that this complex remained stable after drug treatment, while other assembly factors dissociate from the particle. In addition, a reduction of Rok1 levels, compared to untreated cells was observed. However, the reduction after both 2 and 15 minutes was more dramatic than after 30 minutes. It therefore cannot be excluded that the decrease of Rok1 levels is transient and the Rok1 levels accumulate again after prolonged exposure to rapamycin. Moreover, the ribosomal proteins Rpl5 and Rpl16 were detected. Since the Nop58-particle represents a very early pre-ribosome, it was assumed that these were contaminations. This coincides with the finding that hardly any r-protein levels could be detected in samples purified using magnetic beads, as this method is known for obtaining eluates with less impurities (see Figure 8A).

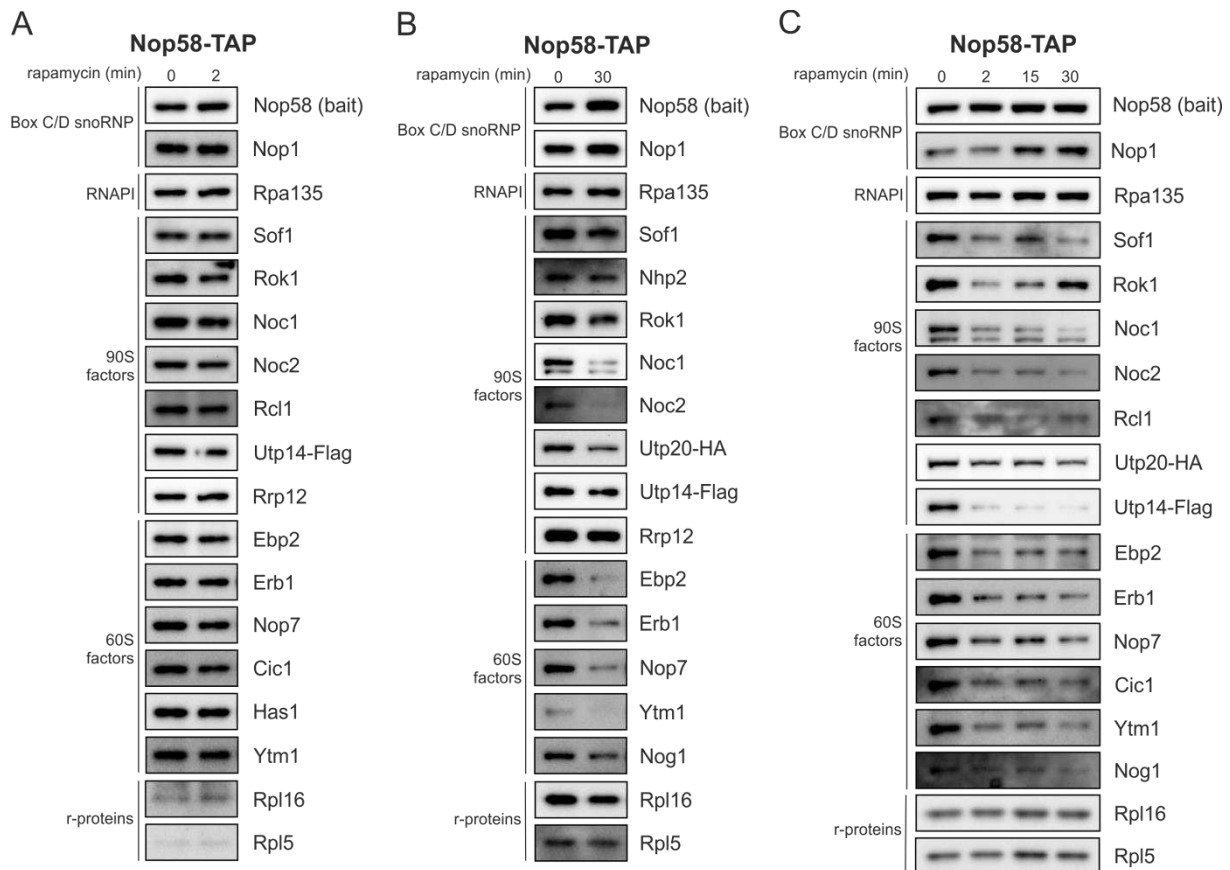


Figure 8: Rapamycin leads to a dissociation of Nop58 containing snoRNP from pre-60S particles. The Nop58-TAP strain expressing *UTP14-FLAG* and *UTP20-HA* (#6616B) was grown to late log phase and treated with rapamycin (3 $\mu\text{g}/\text{ml}$) for 2 to 30 minutes. Nop58-TAP-containing pre-ribosomal particles were then purified by tandem affinity purification using magnetic (A) or IgG (B and C) beads. The analysis of co-purified proteins was performed by western blotting with antibodies directed against selected assembly factors, ribosomal proteins (r-proteins) and the RNA polymerase I (RNAPI). Since antibodies against Nop58, Utp14 and Utp20 were not available, they were detected via the calmodulin binding protein, a flag or an HA tag, respectively.

Northern blotting was done using RNA isolated from crude extract and TEV eluate aliquots from the purified pre-ribosomal particles of the same purifications. Regarding the amounts of total RNA, there was no significant change in the first 15 minutes of rapamycin treatment. However, after 30 minutes of treatment, there were decreased levels of 27S and increased levels of 35S and 23S rRNA observed in the crude extract (Figure 9A). The 27S rRNA is composed of the 27SA₂, the 27SA₃ and the 27SB rRNA. These three pre-rRNAs cannot be resolved by agarose gel electrophoresis. Therefore, the blots were detected with one probe specifically detecting the 27SA₂ rRNA and one probe detecting total 27S rRNA (containing 27SA₂, 27SB and the 27SA₃, which is present only in minor amounts in the cell). The Nop58-particle contained high levels of 27SA₂ and significant amounts of 23S rRNA (Figure 9B and 9C). Since the latter intermediate is generated by direct cleavage of the A₃ site of the primary transcript, its detection in a rapamycin-untreated wild-type strain was unexpected. Under optimal conditions, the 35S primary transcript is predominantly cleaved co-transcriptionally at sites A₀-A₂, producing 20S and 27SA₂ pre-rRNA. However, a small fraction of the processing occurs post-transcriptionally at the A₃ site. The resulting 23S rRNA is obviously contained in a part of the early,

Nop58-TAP containing pre-ribosomes. Furthermore, post-transcriptional A₃ cleavage is increased when cells are exposed to stress or when the cell division rate is slowed (Osheim et al., 2004; Talkish et al., 2016). Although the control sample was not exposed to rapamycin, it was treated with the drug vehicle, DMSO. Whether DMSO increases the fraction of post-transcriptional processing was not investigated. Moreover, mature rRNA was also detected, but it was assumed that these were contaminations as Nop58 is a component of very early pre-ribosomes.

Following longer rapamycin exposure (30 minutes), the levels of 27S rRNA, especially 27SA₂ rRNA, dropped; but 23S rRNA and 35S pre-rRNA could still be detected (Figure 9B and 9C). Thus, the 23S rRNA and to a lesser extent the 35S pre-rRNA were retained in the Nop58-particle during longer periods of drug treatment. Together with the co-purification of Nop1 detected in western blots, these results suggest that Nop58 snoRNP is trapped at the 23S rRNA and possibly at very early stages of rRNA production containing 35S pre-rRNA and RNA polymerase I.

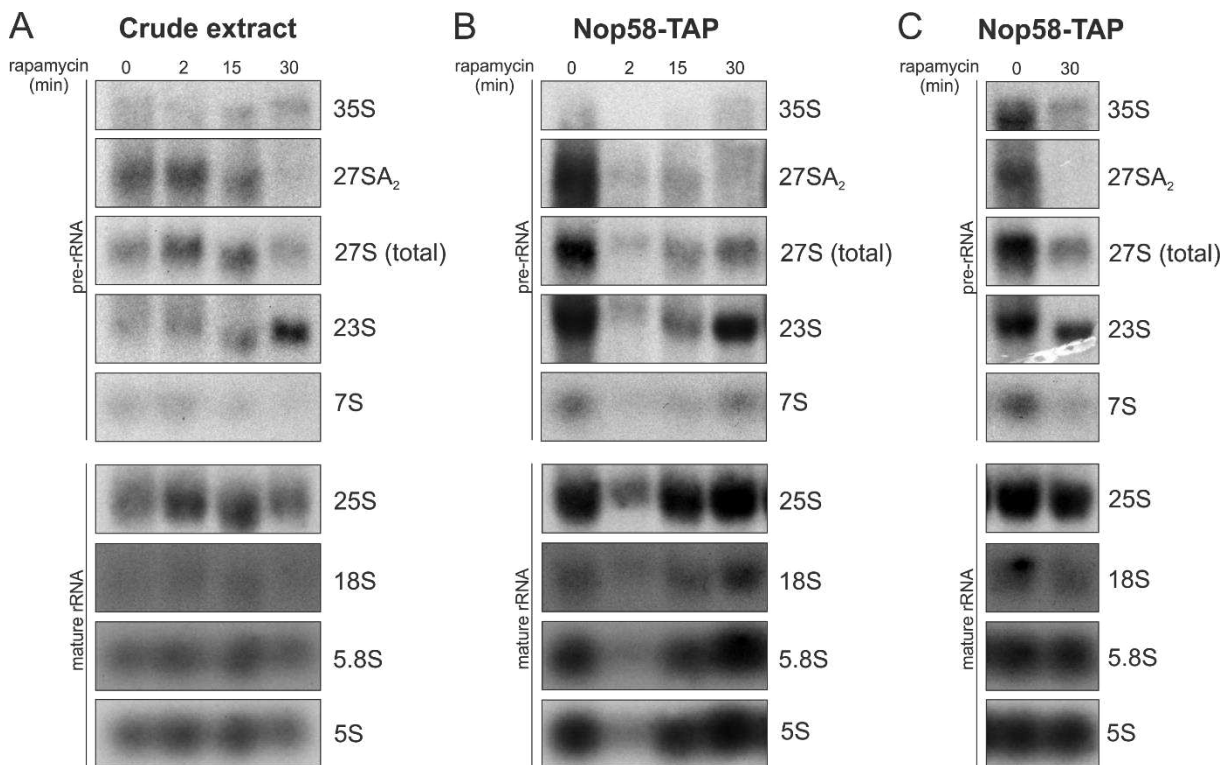


Figure 9: Nop58 is trapped at the 23S rRNA after 30 minutes of rapamycin treatment. The Nop58-TAP strain expressing *UTP14-FLAG* and *UTP20-HA* (#6616B) was grown to late log phase and treated with rapamycin (3 μ g/ml) for 2 to 30 minutes. After isolation of pre-ribosomal particles using Nop58-TAP as bait protein, RNA was extracted using the hot phenol method, separated by agarose gel electrophoresis and analysed by northern blotting using radiolabelled oligonucleotides. The total RNA from the crude extract is shown in (A); RNAs from TEV eluates from two biological replicates are shown in (B) and (C).

3.2 Effect of Rapamycin on the composition of the Noc2-particle

To gain insight about the effect of rapamycin on early pre-60S particles, we purified pre-60S particles using Noc2 as bait protein. This protein is also thought to be recruited to the 35S-pre-rRNA, but stays attached for a longer period of time with the pre-60S particles compared to Nop58 (for references see 1.4). The detection of co-purified RNAs and proteins after 2 and 30 minutes of rapamycin treatment is shown in Figure 10. To monitor whether these compositional changes are specific to TORC1, a strain expressing the mutant *tor1-1*, was also examined. The Tor1-1 protein contains the amino acid exchange at position S1972 that mediates rapamycin resistance (Heitman et al., 1991a; Helliwell et al., 1994).

After 2 minutes of treatment, only minor changes were observed. The amounts of early assembly factors decreased or did not change, while the levels of the later assembly factors (e.g. Erb1, Nop7, Cic1, Nog1, Nsa2 or Noc3) slightly increased (Figure 10A).

After 30 minutes of rapamycin treatment, the Noc2-particle protein composition exhibited dramatic changes (Figure 10B). With the exception of Noc1, Noc3 and Rpa35, all protein levels strongly decreased. The decrease of most pre-ribosome maturation factors was accompanied by a decrease of 27SA₂ pre-rRNA with only small levels of total 35S, 32S and 27S pre-rRNA as well as 23S rRNA remaining (Figure 10C). Clearly, the ratio between 32S and 35S pre-rRNA changed upon drug treatment with 35S becoming the dominant pre-rRNA species. Consistent with a blockage at the 35S pre-rRNA level and the concomitant decrease of 32S pre-rRNA, the 20S pre-rRNA decreased after rapamycin treatment. Since the Noc2-particle represents an early pre-ribosomal complex, the mature rRNAs, which could also be detected, are probably contaminations.

Changes that occurred after 30 minutes of treatment were specific for TORC1, because they were not observed in the rapamycin resistant *tor1-1* mutant. With few exceptions (Erb1, Noc3, Nog1 and Nsa2), this was also true for effects observed in the protein composition of Noc2-particles after 2 minutes of rapamycin treatment. Interestingly, this mutant showed a significantly different particle composition compared to the wild-type strain, with higher levels of very early pre-ribosome maturation factors (Rrp12, Noc1, Sof1 and Rok1) and lower levels of late pre-60S maturation factors (i.e. Nsa2 and possibly also Nog2 and Rsa4). This finding suggests that the mutation leading to the resistant phenotype also affects the functionality of Tor1. Northern blot analysis of the *Tor1-1* strain revealed an accumulation of 32S rRNA (Figure 10C). Furthermore, the contents of 20S pre-rRNA in the *tor1-1* mutant were lower, and the ratio of 27SA₂ and total 27S pre-rRNA clearly shifted towards 27SA₂. All this data indicate a shift to an earlier particle. Because the last factors accumulating in the mutant strain were Ytm1 or/and Nog1, the blockade in 60S ribosome biogenesis seems to take place

somewhere at this assembly step. However, it should be noted that the *TOR1* wild-type strain is not fully isogenic to the *tor1-1* mutant strain. Thus, the possibility of strain-specific differences has to be considered.

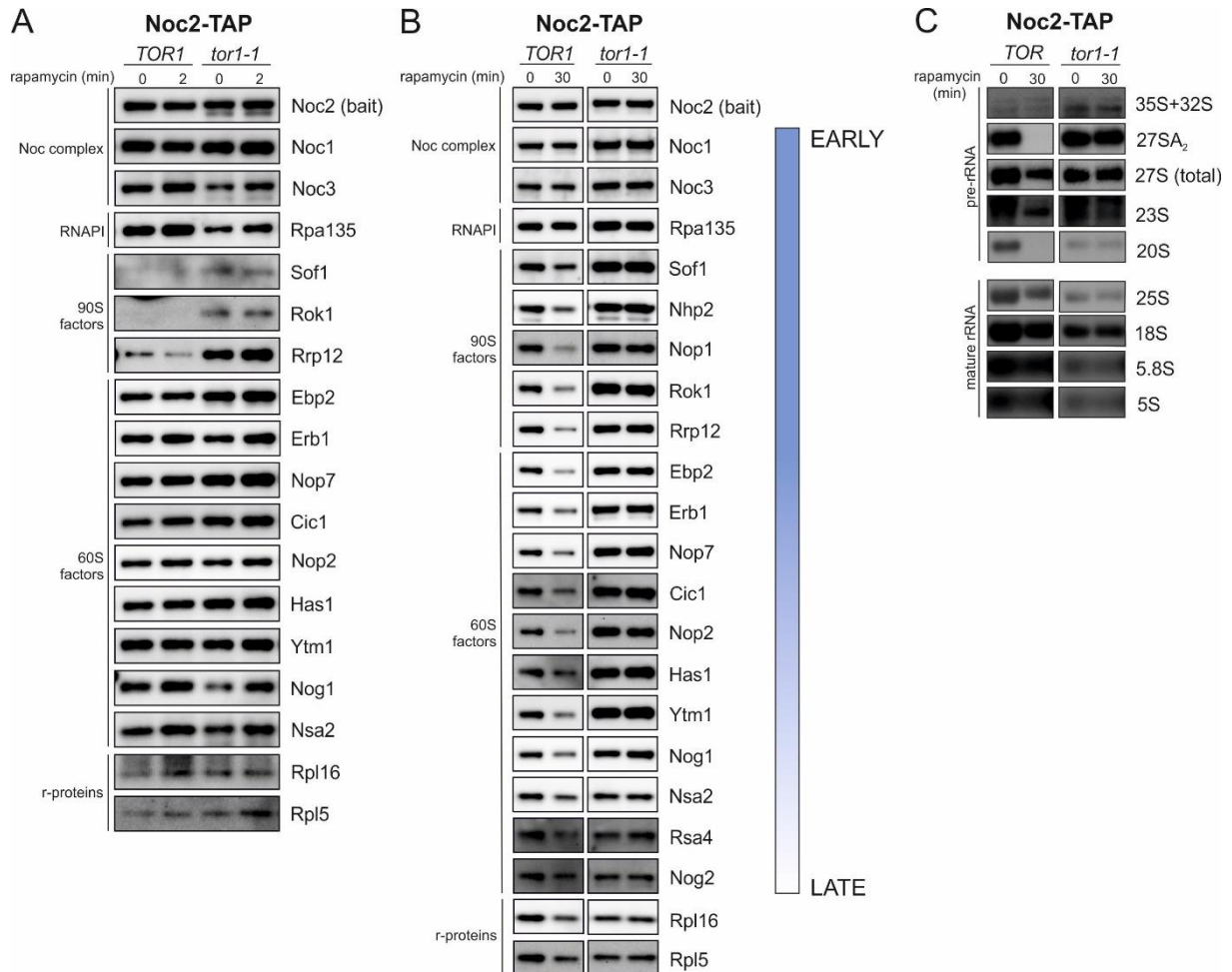


Figure 10: Compositional changes of Noc2-particles in the Noc2-TAP and HHY110 strain before and after rapamycin treatment. Pre-ribosomal particles were purified from the rapamycin-treated *TOR1* wild-type strain (#6616C) and the rapamycin resistant mutant (#6613C). Strains were treated with 3 μ g/ml rapamycin for 2 or 30 minutes. The drug vehicle DMSO served as control. The bait protein was isolated together with co-purified proteins and rRNAs by tandem affinity purification using magnetic (A) or IgG beads (B and C). The components were then analysed by western- (A and B) and northern blotting (C). The proteins detected in the western blots were ordered according their action in the maturation cascade from early to late as symbolized by a vertical bar shown in (B).

Since the 27SA₂ rRNA was missing in Noc2-particles and the amount of total 27S rRNA was not significantly altered, these data suggest that Noc2 remains part of a later particle in the *TOR1* wild-type strain upon rapamycin treatment. This is in agreement with increased levels of later assembly factors, which were observed in particles exposed to rapamycin for 2 minutes.

3.3 Impact of hyperactive *tor1*^{L2134M} variant on pre-ribosomal particle composition

To gain a further insight into the impact of TORC1 on early ribosome biogenesis, a hyperactive *tor1* mutant strain and its isogenic wild-type strain expressing a *TAP*-tagged *NOC2* were constructed. The mutant possesses a leucine to methionine amino acid exchange at position L2134, which is located within the kinase domain of Tor1 (Takahara and Maeda, 2012). Isolation of corresponding Noc2-particles and subsequent detection of co-purified proteins by TAP purification and western blotting were performed by Gertrude Zisser. The detection of co-purified proteins after 2 and 30 minutes of rapamycin treatment is shown in Figure 11.

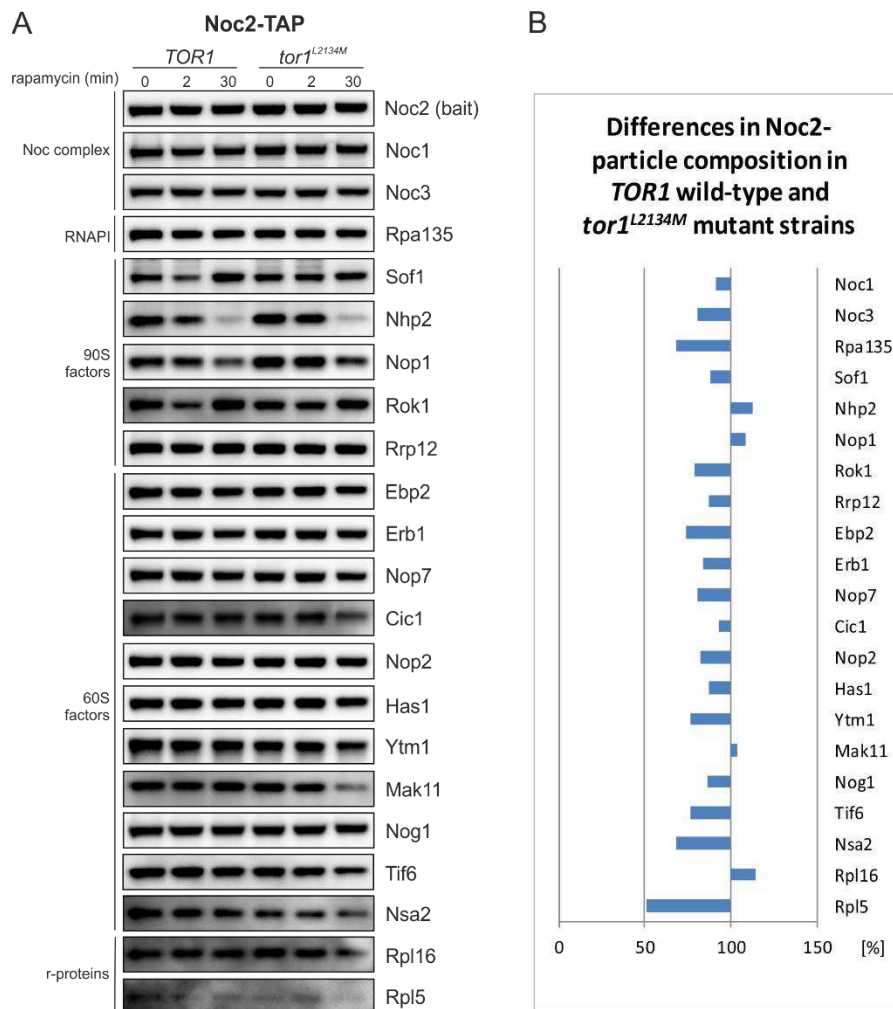


Figure 11: Behaviour of Noc2-particles in a hyperactive *tor1*^{L2134M} mutant strain in the absence and presence of rapamycin. A hyperactive Tor1 strain (#6678D) and its isogenic wild-type strain (#6678B) expressing a *TAP*-tagged *NOC2* were exposed for 2 and 30 minutes to rapamycin (3 µg/ml). Pre-ribosomal particles were TAP purified using magnetic beads and analysed for co-purified proteins (A). This experiment was performed by Gertrude Zisser. A semi-quantitative analysis of the western blot results, which represents the changes in Noc2-particle composition of the hyperactive *tor1*^{L2134M} mutant compared to the *TOR1* wild-type strain (in %) is illustrated in (B). Values from 0 to 100 % denote a decrease whereas values above 100 % denote an increase of respective factors.

Consistent with the above shown data, the levels of the snoRNP proteins Nop1 and Nhp2 in Noc2-particles decreased rapidly in the rapamycin-treated wild-type strain (Figure 11A). Interestingly, the hyperactive *tor1* mutant showed significantly higher levels of these proteins than the wild-type strain. Moreover, the proteins decreased more slowly in the presence of rapamycin. Further effects of rapamycin on the composition of Noc2-TAP containing particles in the *TOR1* wild-type strain concerned the 90S factors Sof1 and Rok1, whose levels temporarily dropped after 2 minutes of treatment, but recovered after 30 minutes of treatment.

Taken together, these results suggest that TORC1 affects the association of the snoRNPs with the pre-ribosomal particles and that the blockade takes place in early assembly stages after Rok1 and Sof1 binding.

In order to perceive possible changes caused by the *tor1*^{L2134} mutation, the untreated mutant was compared with the untreated wild-type strain. A semi-quantitative analysis (Figure 11B) revealed a reduction of most assembly factors. Exceptions were Nhp2 and Nop1, whose levels accumulated, and Mak11, whose protein level hardly changed. In addition, the r-protein Rpl16, which assembles at the stage of the Noc2 containing particle (Zisser et al., 2018), accumulated. Thus, it is possible that the blockade caused by the *tor1*^{L2134} mutation takes place shortly after this assembly step.

3.4 TORC1 inactivation does not influence Noc2 localisation

Since TORC1 inactivation leads to a delocalisation from the nucleolus of the assembly factor Nop58 into the nucleoplasm (Kakihara et al., 2014), we asked whether the localisation of Noc2 is also influenced by rapamycin treatment. For this purpose, a strain with a *GFP*-tagged *NOC2* and a *mCherry*-tagged *NOP58* was examined by fluorescence microscopy (Figure 12). Nop58-mCherry diffused into the nucleoplasm upon TORC1 inactivation, confirming the results from Kakihara et al., 2014. Noc2-GFP was present in the nucleolus both before and after rapamycin treatment, suggesting that the Tor1 kinase has no effect on its localisation. However, in contrast to Milkereit et al. no clear nucleoplasmic localisation of Noc2 (Milkereit et al., 2001) could be determined in the untreated strain. However, due to the small structure of the nucleolus, small changes in localisation are difficult to judge. In order to determine whether there is really an unmixing of the Noc2 and Nop58 signals upon rapamycin treatment, the strain should be analysed in a more quantitative manner by high resolution laser scanning microscopy.

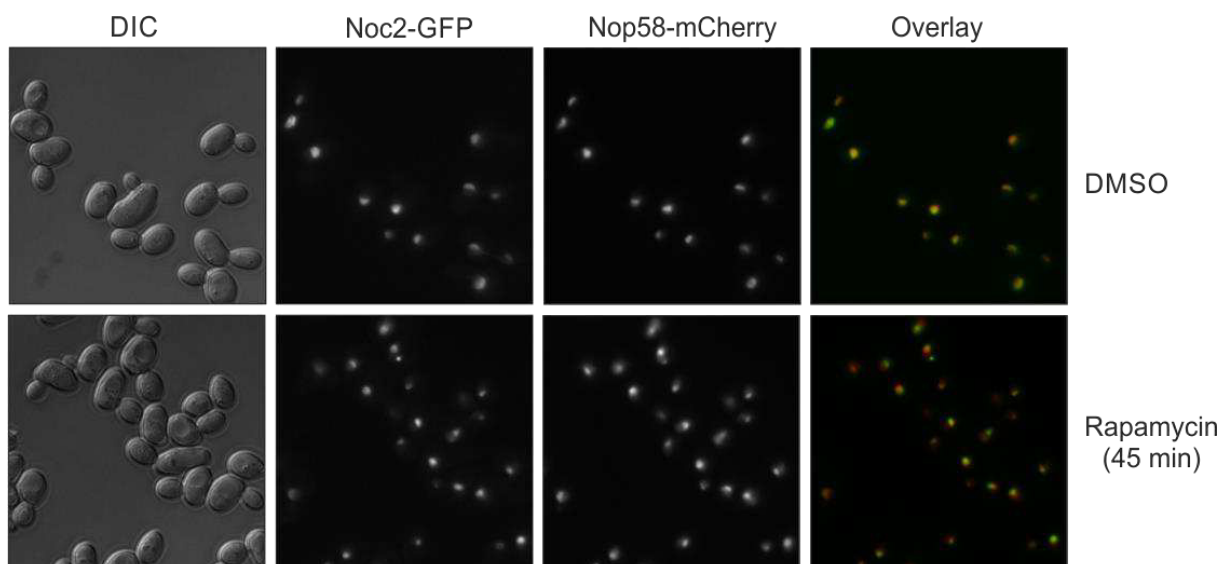


Figure 12: *In vivo* localisation of Noc2-GFP and Nop58-mCherry in untreated and rapamycin-treated *Saccharomyces cerevisiae* cells. A GFP- and mCherry-tagged strain (#6594D) was exposed to rapamycin (3 $\mu\text{g/ml}$) or to the equivalent concentration of the drug vehicle DMSO. The strain was analysed for its GFP and mCherry fluorescence. Sections of DIC, GFP, and mCherry images are shown. In addition, an overlay of the GFP (green) and mCherry (red) image was created.

3.5 Effects of TORC1 inhibition on intermediate and in late nucleolar pre-ribosomal particles

The previous data of this study demonstrated that yeast cells experience a lack of 27SA₂ pre-rRNA upon long TORC1 inactivation in *TOR1* wild-type strains (Figure 9A). However, Nop58 as well as Noc2 associates with pre-rRNA before 27SA₂ rRNA formation. For this reason, assembly factors that bind nucleolar pre-ribosomal particles after the A₂ cleavage step became more interesting for this study.

The Nsa1-particle is a specific intermediate, which presents a late nucleolar pre-66 particle. This pre-ribosomal complex is known for its almost exclusive association with the 27SB rRNA (Kressler et al., 2008). Northern blot analysis of TAP-purified Nsa1-particles revealed a clear signal of total 27S pre-rRNA, but also small amounts of 27SA₂ rRNA (Figure 13C). Since this pre-ribosomal particle isolation was based on a one-step TAP purification using IgG beads, this could be a contamination. Nevertheless, an interesting effect was observed in the data showing the composition of Nsa1-particles after long rapamycin treatment. 30 minutes of drug treatment led to a distinct accumulation of total 27S rRNA and to the disappearance of 27SA₂ rRNA. In addition, 35S, 32S and 23S rRNA increased slightly. An accumulation of mature rRNA was also noticeable. But since the 18S rRNA – a component of the 40S ribosome subunit – was also significantly increased, it was assumed that this effect was due to an unequal RNA loading on the gel.

In aliquots of the same sample, all investigated assembly factors and r-proteins decreased markedly upon long TORC1 inactivation (30 minutes) (Figure 13B). The RNAPI also showed a clear reduction in relation to the bait protein. After 2 minutes of rapamycin treatment (Figure 13A), primary effects were observed that differed from the secondary effects. There were already some factors which were reduced (Nop7, Cic1, Ytm1, Noc3 and Nsa2), but another factor, the shuttling protein Nog1, increased. Interestingly, Nog1 was proposed previously to be regulated by the TORC1 pathway (Honma et al., 2006).

Taken together, these data suggest that after prolonged TORC1 inactivation, maturation factors dissociate from the Nsa1-particle and the majority of Nsa1 is trapped at 27SA₃ or/and 27SB rRNA.

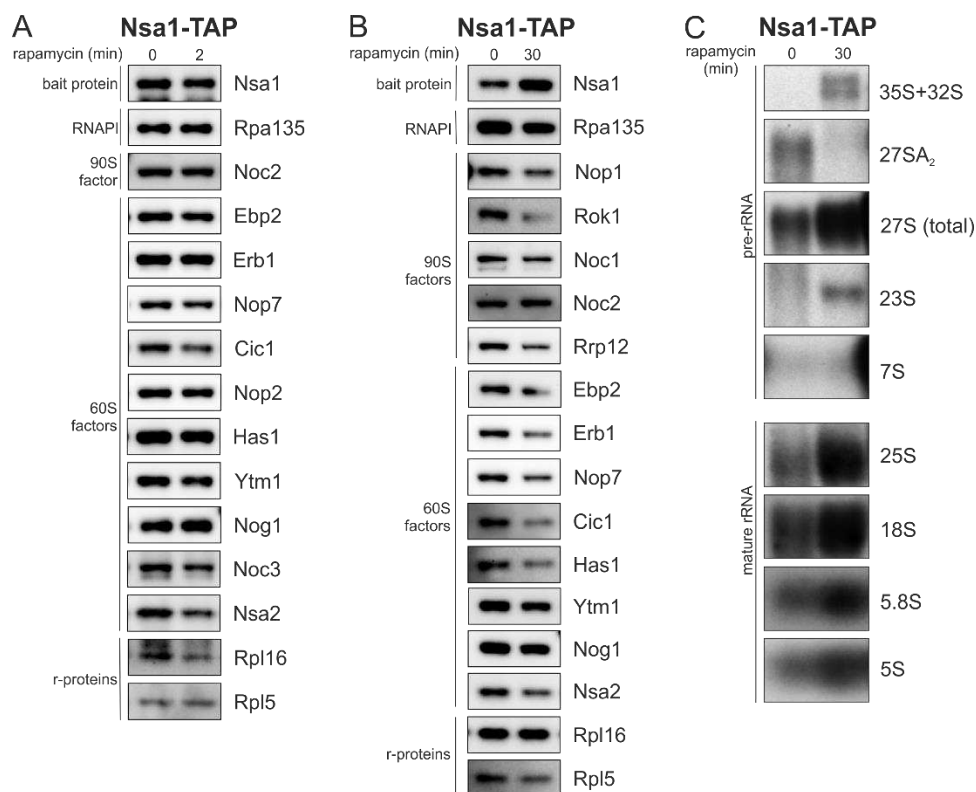


Figure 13: Nsa1 is trapped at 27SA₃ and/or 27SB rRNA after rapamycin treatment. For tandem affinity purification, magnetic (A) and IgG beads (B and C) were used to isolate Nsa1-TAP and its bound components from the rapamycin (3 µg/ml) treated strain (#6393). TEV eluates samples were analysed by western and northern blotting.

The GTPase Nog1 is a shuttling protein and assembles into early pre-ribosomal particles containing 27SA₂ rRNA, but remains associated until late 66S-particles are formed (Kressler et al., 2010; Saveanu et al., 2003). As expected, TAP purified Nog1-particles showed high levels of 27S pre-rRNA, 7S pre-rRNA, 25S rRNA and 5.8S rRNA, and showed only low levels of 35S pre-rRNA. 23S pre-rRNA was observed in Nog1-particles shown in Figure 14B, but not in Nog1-particles shown in Figure 14E. This could be due to better RNA isolation in connection with a long exposure time. After 2 minutes of rapamycin treatment there was a slight accumulation of 35S rRNA and 32S rRNA, which was more pronounced after 30 minutes of drug treatment. In addition, it seemed that there was a slight in-

crease of total 27S rRNA and 7S rRNA. However, RNA amounts of TEV eluates could not be determined and adjusted due to their low concentration. It must therefore be taken into account that this could also be the result of unequal RNA loading on the gel. In contrast, after 30 minutes of drug treatment, the Nog1-particles showed a dramatic decrease in the amounts of 27S and 7S rRNA.

Different changes occurred in the protein composition of the Nog1-particle after 2 (Figure 14C) and 30 minutes (Figure 14D) of rapamycin treatment. Fast effects included a decrease of Noc1 and Nog2 and an increase of Erb1 and Noc3. Other protein levels barely changed after 2 minutes of drug treatment. Long drug exposure (30 minutes) caused a decline in almost all assembly factors. The majority of early factors decreased more drastically than later ones. Exceptions were Sof1 and Rok1, which were difficult to detect, but were present in unchanged quantities. Furthermore, Nhp2, a member of the H/ACA snoRNPs, which is required for the maturation of the 18S rRNA (Henras et al., 1998), was increased in the presence of rapamycin.

These data indicate that most of the Nog1 protein becomes soluble after long time rapamycin treatment. It seems that a small part remains in particles, which contain 35S or 32S pre-rRNA. This is consistent with the finding that the protein levels of Sof1, Rok1 and Nhp2 remained unchanged or accumulated. Also, the levels of Rpa135 did not drop completely. Nsa2, Nog2, Rsa4 and Drg1 are 60S factors, which associate with pre-ribosomal particles in later maturation phases (Konikkat and Woolford, 2017). Their less pronounced decrease suggest that during 30 minutes of treatment later particles persist or that those late particles that are still in course of transition through the maturation cascade after blocking early maturation steps by rapamycin treatment. This situation is comparable to that after diazaborine treatment, where also after longer treatment periods, the particle composition changed to later stages (Zisser et al., 2018). Consistent with the presence of later particles in the Nog1-TAP preparation, mature rRNAs were still present or increased (5.8S rRNA) in Nog1-particles exposed to rapamycin.

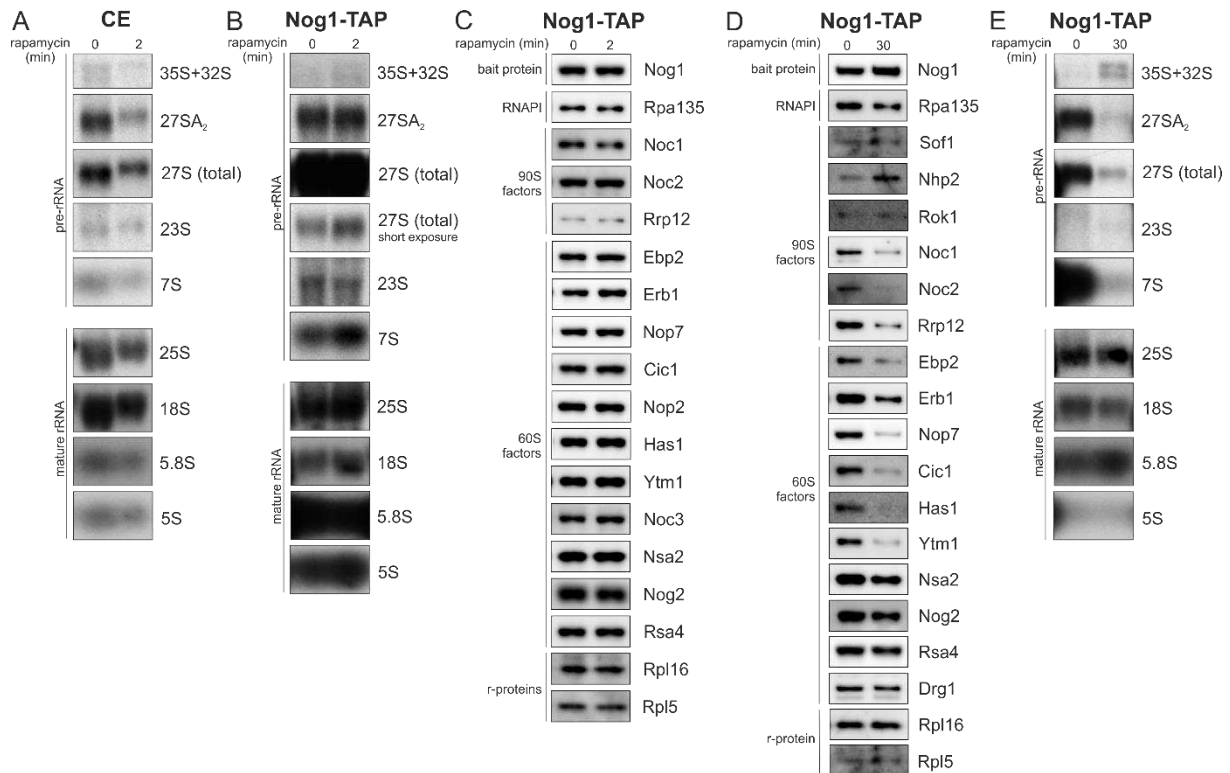


Figure 14: Early and late effects in the RNA and protein composition of *Nog1*-particles. Two litres of cell cultures of a *Nog1-TAP* strain (#6393) were cultured until an OD₆₀₀ between 1.0 and 1.3. DMSO was then added to the "untreated" strain and rapamycin was added to the treated strains in a final concentration of 3 µg/ml. *Nog1*-particles exposed for 2 minutes to rapamycin were purified via magnetic beads and *Nog1*-particles exposed for 30 minutes to rapamycin were purified via IgG beads according to the TAP protocol (see 2.3). Proteins and rRNAs of crude extracts (CE) and TEV eluates were detected by western and northern blotting.

3.6 There are serine-phosphorylated proteins in Nop58-, Noc2-, *Nog1*- and Nsa1-particles

As shown in the previous chapters, TORC1 influences the composition of early and late nucleolar particles in the ribosomal assembly pathway. Because the phosphatidylinositol kinase Tor1 phosphorylates serine and threonine residues of its target proteins, an antibody directed against phosphoserine was used to identify possible substrates in the early 60S ribosome assembly pathway. The membranes showing the respective signals and the corresponding SDS PAGE gels are shown in Figures 15 and 16.

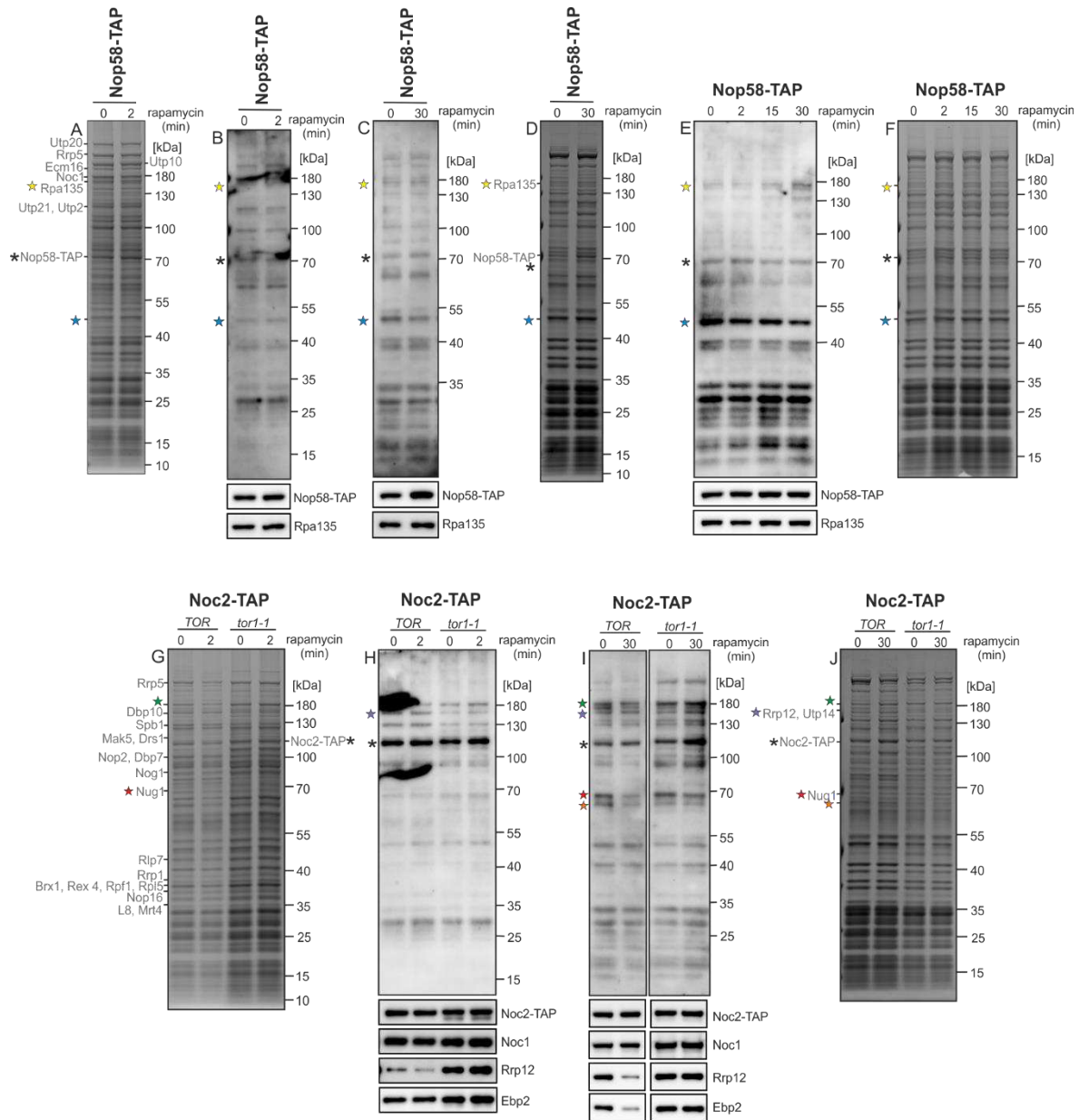


Figure 15: Protein composition and serine-phosphorylated components of very early pre-ribosomal particles. Cultures of Nop58-TAP and Noc2-TAP strains were exposed to rapamycin (3 $\mu\text{g}/\text{ml}$). After tandem affinity purification using magnetic (A/B and G/H) or IgG beads (C/D, E/F and I/J) the particles were examined for their protein content by SDS PAGE and for possible serine-phosphorylated proteins by western blotting using a phosphoserine specific antibody. The membranes (B, C, E, H, I and L) are arranged in close proximity to their corresponding SDS PAGE gels (A, D, F, G and J). Note that none of the protein bands of the gels were identified by mass spectrometry analysis. The protein labelling is based on previous mass spectrometry analyses of Nop58- and Noc2-particle bound components purified by Gertrude Zisser. The * symbol indicates the possible position of the corresponding bait protein; stars point to interesting changes or to issues that are addressed in the text.

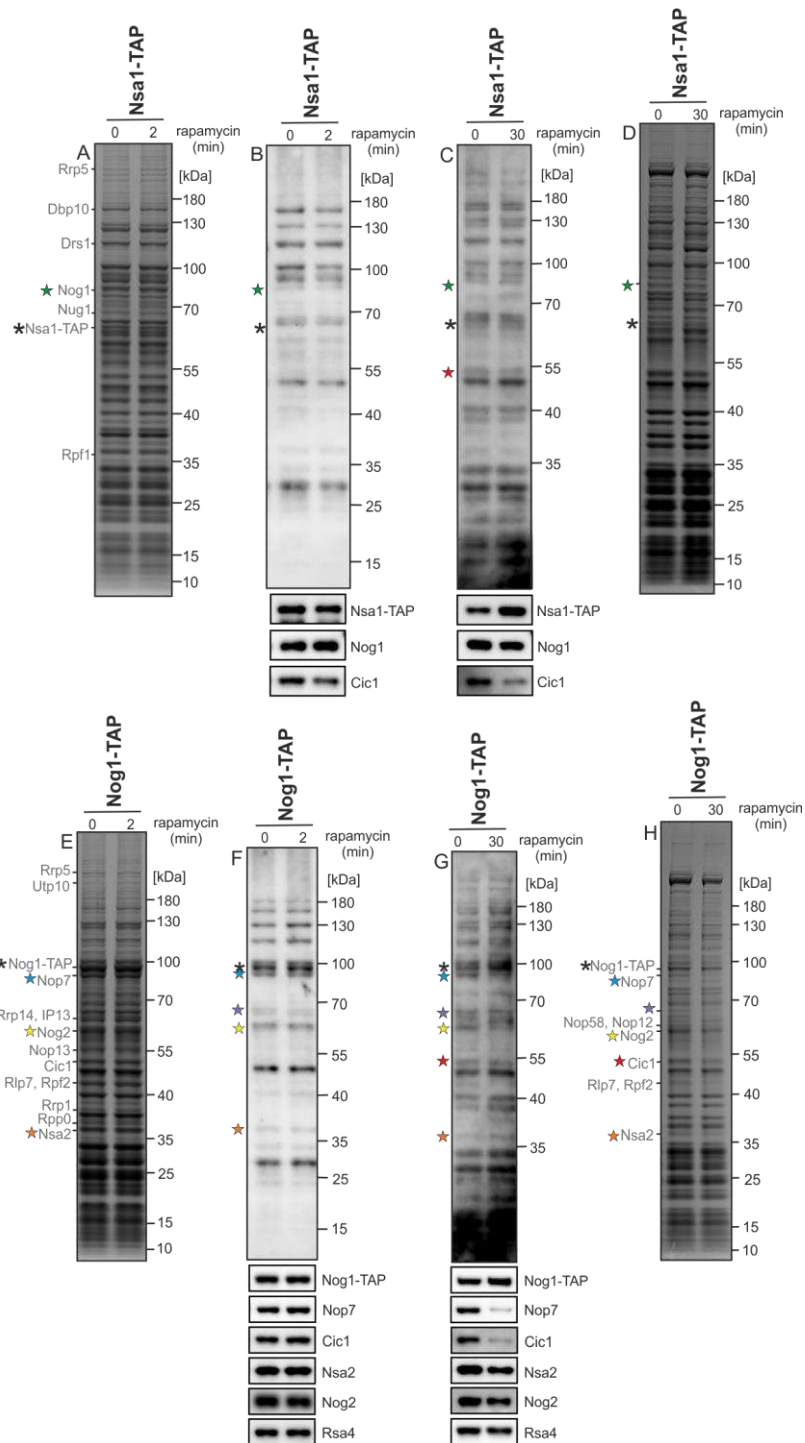


Figure 16: Protein composition and serine-phosphorylated components of late nucleolar pre-ribosomal particles. Pre-60S particles from rapamycin (3 $\mu\text{g}/\text{ml}$) treated and untreated Nog1- and Nsa1-TAP strains were isolated by tandem affinity purification using magnetic (A/B and E/F) or IgG beads (C/D and G/H). The particles were then examined for their protein content by SDS PAGE and for possible serine-phosphorylated proteins by western blotting using an antibody directed against phosphoserine. The membranes (B, C, F and G) are arranged in close proximity to their corresponding SDS PAGE gels (A, D, E and H). It has to be noted that no mass spectrometry analysis of these gels has been done. The protein labelling is based on previous mass spectrometry analyses of Nsa1- and Nog1-particle bound components purified by Gertrude Zisser. The * symbol indicates the possible position of the corresponding bait protein; stars point to interesting changes or to issues that are addressed in the text.

After antibody detection, the membranes showed multiple protein bands of different intensities. Some of these signals decreased noticeably after long periods of rapamycin treatment. Two exam-

ples marked with a blue and a yellow star can be found on membrane G in Figure 16. Based on the comparison with previous mass spectrometry analyses, these signals showed a similar migration behaviour in SDS-PAGE as bands identified as the assembly factors Nop7 (blue star) and Nog2 (yellow star). However, since western blot analysis had already shown that the protein amounts of these factors decrease after 30 minutes of drug treatment (see Figure 14E or the section below the respective phosphoserine detected membrane), the reason for the lack of phosphoserine signal is probably the absence of these proteins in Nog1-particles. Three more examples of such eye-catching changes were also found in Nop58-particles (Figure 15C and 15E; see blue star) and in Noc2-particles of the *TOR1* wild-type strain (Figure 15I; see red and orange star). One of the signals might be Nug1 (red star); another could be the r-protein Rpl3 (blue star). Since no specific antibodies for these proteins were available, it is not possible to make a statement about their phosphorylation state. It is worth mentioning that the phosphoserine signal assigned to Rpl3 was also found in other particles, but did not decrease there (Figures 15CEHI and 16BCFG). Due to its running behaviour, the third signal could be Ebp2 (orange star). Its protein level also disappeared in Noc2-particles treated with rapamycin, but was clearly present in the *tor1-1* mutant strain. However, its phosphoserine signal in the mutant strain became weaker. Consequently, the assembly factor Ebp2 in *tor1-1* mutants is probably less phosphorylated.

These data showed that the present phosphorylation states of some proteins did not seem to be caused by TORC1. This was also true for protein bands thought to be the bait protein in Noc2-particles, which were clearly phosphorylated but showed no changes in the phosphoserine signal following rapamycin treatment (Figure 15H and 15I). This is in contrast with the data of A. Cremonesi's dissertation, who reported a TORC1 dependent phosphorylation of Noc2 (Cremonesi, 2002).

Of particular interest for the purpose of recognition of possible TORC1 substrates, were phosphoserine signals that behave differently to their existing levels in pre-ribosomal particles. In fact, such cases were found on several membranes, but could only be detected after 30 minutes of rapamycin exposure. For a better comparison, the western blot detections of the corresponding proteins are shown below the membranes of Figures 15 and 16:

- Membrane 15E showed a band just below the 180 kDa marker of the protein standard (yellow star), whose intensity was increased after 30 minutes of drug treatment. Rpa135 is also positioned at this height, but its protein level did not change in Nop58-particles in neither the absence nor presence of rapamycin. The same band was also slightly increased in membrane 15C.
- Noc1 is a factor that also did not change in Noc2-particles of one of the *TOR1* wild-type strains. The proteins can be detected at 180 kDa. At the same high and on the same membrane (Figure 15I) a slightly decreased phosphoserine signal was present (green star).

- The constant signal next to the violet star on the same membrane possibly corresponds to Rrp12 and/or Utp14. Utp14 could not be detected in Noc2-particles, but Rrp12 showed a notable decrease.
- Moreover, a possible Nog1 phosphoserine signal was observed in Nsa1- (Figure 16C; see green star) and Nog1-particles (Figure 16F and 16G; see symbol *). These phosphoserine signals seemed to increase after long exposure to rapamycin. Interestingly, it has already been shown that the kinase Tor1 affects the shuttling protein Nog1 (Honma et al., 2006).
- Phosphoserine signals, which were migrating in SDS-PAGES similar to Cic1 and Nsa2, are indicated in Figure 16G (Nog1-TAP) by a red and orange star, respectively. While the amounts of Cic1 and Nsa2 in Nog1-particles decreased after 30 minutes of rapamycin treatment, the phosphoserine signals either increase or did not change. Possible Cic1 phosphoserine signals that behave differently to their levels in pre-ribosomal particles were also found on membranes 15I (Noc2-TAP) and 16C (Nsa1-TAP). However, Cic1 was hardly present in these rapamycin-treated strains, suggesting that the phosphoserine signal arises from a different protein.
- Another interesting phosphoserine signal of the Nog1-TAP strain is located below the 70 kDa marker of the protein standard (Figure 16G; see violet star). The comparison with the running behaviour of detected co-purified proteins indicated that this could be Rsa4.

Taken together, these data suggest a number of possible TORC1 substrates. Therefore, it would well be worth to identify the proteins represented by these phosphorylated bands using mass spectrometry.

Western blot analysis revealed another interesting aspect that can be seen in Figures 15H and 15I. The effect refers to the bait protein Noc2 in the *TOR1* wild-type and in the *tor1-1* mutant strain. The comparison of the migration of Noc2 in particles isolated from these two strains showed that Noc2 is migrating significantly slower in the rapamycin resistant strain. This was observed in detections of phosphoserine and Noc2 via directed antibodies, which strongly suggests that the corresponding phosphoserine signal indeed belongs to Noc2. It further indicates a possible modification difference of Noc2 in the *tor1-1* mutant strain.

3.7 Subcellular localisation of late nucleolar pre-60S assembly factors in the absence and presence of rapamycin

As mentioned above, the late nucleolar factors Nsa1 and Nog1 showed changes in protein composition after rapamycin treatment. In order to find out whether other nucleolar assembly factors than Noc2 or Nop58 changed localization in the presence of rapamycin, a number of GFP- and YFP-tagged strains were treated and analysed for their fluorescence. Sections of the respective DIC and GFP or YFP images are shown in Figure 17.

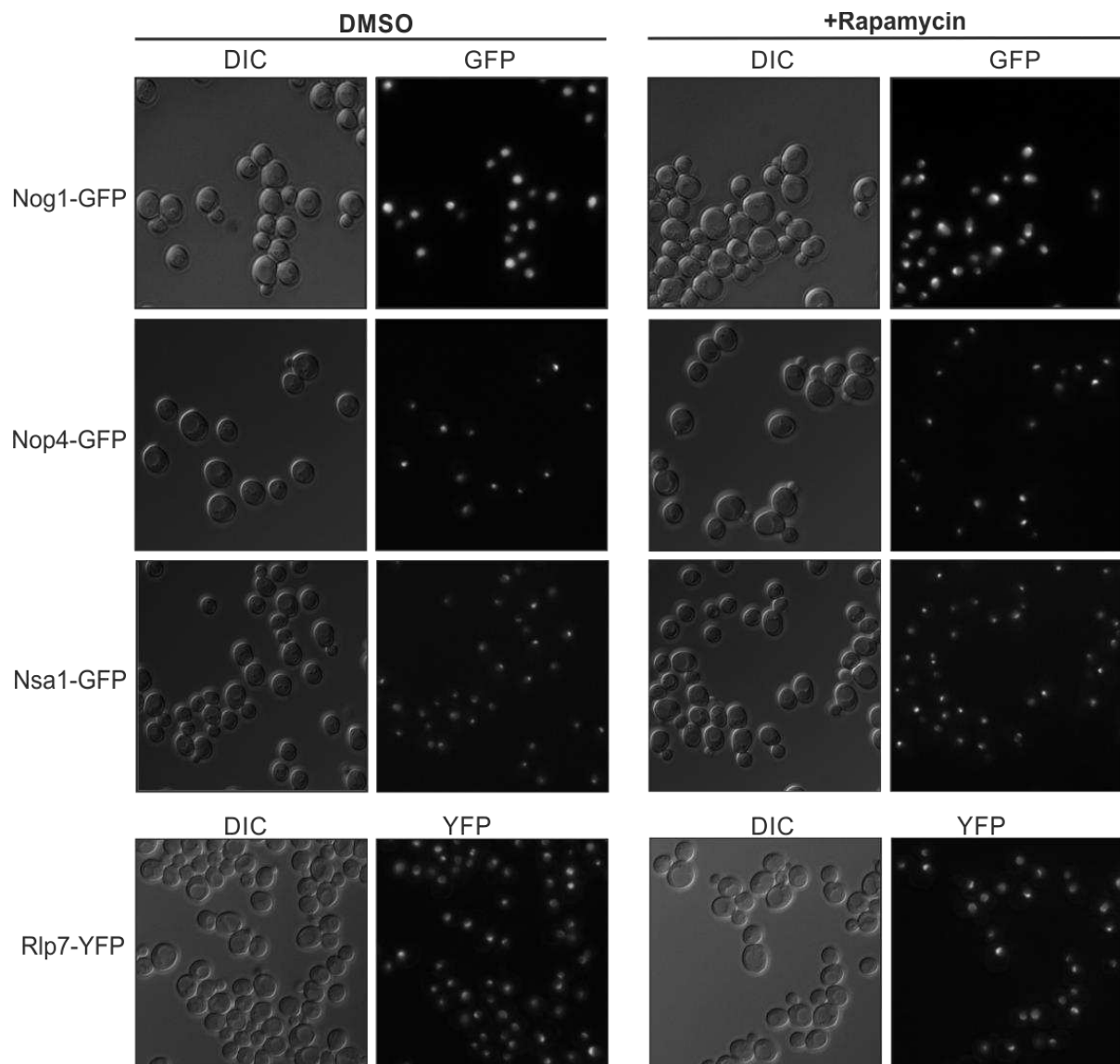


Figure 17: Effect of rapamycin on the subcellular localisation of several 60S assembly factors. Strains expressing GFP- or YFP-tagged *NOG1*, *NOP4*, *NSA1* or *RLP7* (#6008, #6589D, #6590C and #6591C) were treated with rapamycin (3 µg/ml) or its drug vehicle DMSO. Analysis was performed by fluorescence microscopy. The images of DIC and GFP or YFP are shown.

Since it is already known that Nog1 delocalizes in the presence of rapamycin (Honma et al., 2006), a Nog1-TAP strain served as control. Its fluorescence signal was found in almost equal amounts in both

the nucleolus and the nucleoplasm, but upon TORC1 inactivation it was clearly enriched in the nucleus. This was consistent with the data of Honma et al., 2006. However, the other 60S assembly factors studied (Nop4, Nsa1 and Rlp7) showed no pronounced changes in their subcellular localisation. All three of them were located in the nucleolus in both the absence and presence of rapamycin.

4 Discussion

4.1 Particle-specific compositional changes after long-term treatment with rapamycin

The changes in the composition of total RNA after rapamycin treatment detected in this work are comparable to the data of Kos-Braun et al. (Kos-Braun et al., 2017). Although a substantially higher final concentration of rapamycin was used in this study, the effects were also best seen after longer drug treatment (Figure 9A and 14A). The appearance of the 23S and the disappearance of the 27SA₂ rRNA intermediates implies that the 35S primary transcript is cleaved at the A₃ instead of the A₂ site. In addition, the accumulation of the 35S primary transcript indicates defects in its processing. As a result of the alternative processing pathway, the rRNA and protein composition of the pre-ribosomal particles must also change. As the data of this study demonstrated, these changes are unique for each pre-ribosomal particle purified with Nop58, Noc2, Nsa1 or Nog1 as bait proteins.

Nop58 was trapped at the 23S rRNA after rapamycin treatment (Figure 9B and 9C). Since Nop58 is a component of the U3 snoRNP, which associates with the SSU processome near the 5'ETS (Barandun et al., 2017), Nop58 does not seem to be able to dissociate from its binding site when cleavage occurs in A₃ instead at site A₂. Because Nop1 also remained in Nop58-particles upon TORC1 inactivation (Figure 8), it is likely that the entire U3 snoRNP complex persists. The dissociation of U3 snoRNA requires the helicase Dhr1, which is recruited and activated by Utp14 and Bud23 (Sardana et al., 2015; Zhu et al., 2016). In fact, Utp14 levels in Nop58-particles dropped dramatically in the presence of rapamycin. In addition, a phosphoserine signal possibly corresponding to Utp14 was detected in Noc2-particles (Figure 15H and 15I; see violet stars). Unfortunately, western blot analysis showed no signal for Utp14 in Noc2-particles; therefore, the phosphorylation state could not be determined. Nevertheless, these data provide interesting insights. If U3 is indeed not released from pre-ribosomal particles, this defect may be responsible for the failure or the delay in A₂ cleavage. For instance, it has already been shown that the deletion of *UTP14*, *BUD23* or a catalytically inactive *dhr1* mutant leads to defects in A₂ cleavage (Sardana et al., 2013, 2015; White et al., 2008; Zhu et al., 2016). Thus, further investigations concerning the U3 snoRNP, Dhr1, Bud23, and Utp14 are of interest.

Noc2-particles of strains exposed to rapamycin for 30 minutes predominantly contained 27S, but lacked 27SA₂ rRNA (Figure 10C). Since no primer extension experiments were performed to distin-

guish the 27SB from the 27SA₃ rRNA, it remained unclear whether these Noc2-particles contain both rRNA intermediates or not. Post-transcriptional cleavage at A₃ generates 27SA₃ rRNA, which is immediately processed to 27SB rRNA (Kos-Braun et al., 2017). Thus, it is likely that Noc2-particles contain 27SA₃ as well as 27SB rRNA, but 27SA₃ is present in a smaller amount.

In this study western blot analyses of two different rapamycin-treated *TOR1* wild-type strains expressing a *TAP*-tagged *NOC2* were performed. The effects of rapamycin on particle composition were more pronounced in the first Noc2-TAP strain shown in Figure 10. This strain showed the decrease of almost all assembly factors after 30 minutes of rapamycin treatment. In contrast, the snoRNP proteins Nhp2 and Nop1 were the only assembly factors that dropped in the second Noc2-TAP strain (Figure 11) under the same conditions. As the first of the *TOR1* wild-type strains (#6616C) contains more auxotrophies than the second (#6678B, see Table 1), this could correlate with data showing the first *TOR1* wild-type strain to be more sensitive to rapamycin (compare Figure 10B to 11A).

Moreover, Noc2-particles from strains treated for 30 minutes with rapamycin still contained unchanged amounts of Noc1 and Noc3. Levels of all other 90S and 60S factors decreased in the particles from the *TOR1* wild-type strain, which showed greater rapamycin sensitivity. Since Noc2 can be found in a complex either with Noc1 or Noc3 (Milkereit et al., 2001), it is possible that a part of the Noc2 molecules might be dissolved and present as a component of a Noc-complex in the nucleolus (Figure 12) upon long TORC1 inactivation.

Figure 18 provides a model proposing the whereabouts of the early nucleolar assembly factors Nop58 and Noc2 in the rRNA processing pathway after 30 minutes of treatment with rapamycin. Under optimal conditions, Nop58 and Noc2 are recruited co-transcriptionally to the 35S primary transcript, and the separation of 40S and 60S rRNA precursors occurs mainly via the A₂ cleavage step. The assembly factors can then be found at 27SB rRNA, wherefrom they are recycled. Under stress conditions, like in the presence of rapamycin, the 35S primary transcript is mainly processed post-transcriptionally at the A₃ site. Nop58 is then trapped at 23S rRNA, which is an rRNA intermediate produced by the alternative processing pathway. The recycling of Nop58 is consequently no longer possible. Noc2 is partly present at 27SA₃ and/or at 27SB rRNA and partly soluble in a complex with other Noc-proteins.

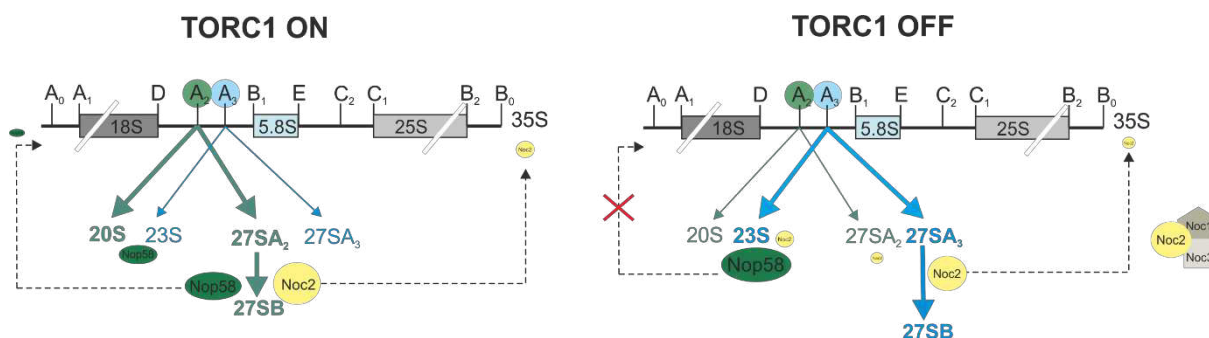


Figure 18: A model depicting Nop58 and Noc2 in A₂ (left) and A₃ (right) processing pathways. Pre-rRNA products of the A₂ processing pathway are shown in green; while those of the A₃ processing pathway are shown in blue. The size of the assembly factors Nop58 (green circles) and Noc2 (yellow circles) reflects the amount of associated rRNA intermediates found in the respective particles.

As described above, post-transcriptional processing at the A₃ site results in a drop in 27SA₂ pre-rRNA. It can therefore be assumed that factors normally associating with 27SA₂ rRNA lose their binding site when the pre-rRNA is cleaved at A₃ instead at A₂, and become soluble. This could explain why the majority of proteins and pre-rRNA components of Nog1-particles decreased dramatically when exposed to rapamycin for 30 minutes (Figure 14D and 14E), indicating a significant portion of free Nog1 bait protein.

In contrast, Nsa1 associates with pre-ribosomal particles containing 27SB pre-rRNA (Kressler et al., 2008). Thus, Nsa1 was found trapped at 27SA₃ and/or 27SB pre-RNAs in Nsa1-particles (Figure 13). However, the effects in Nog1- and Nsa1-particles caused by rapamycin treatment should be reproduced.

In summary, there are clear indications that the TORC1 pathway interferes with the assembly of snoRNPs with pre-ribosomal particles. Noc2-particles showed a significant decrease of the snoRNP compartments Nop1 and Nhp2 (Figure 10 and 11). On the one hand, this is due to the entrapment of Nop1 at the 23S rRNA which was shown for Nop58-particles (Figure 8 and 9). Nhp2, on the other hand, was found enriched in Nog1-particles, most likely in the small particle fraction containing 35S, 32S pre-rRNA or residual 27S pre-rRNA (Figure 14).

4.2 Role of selected factors in ribosomal biogenesis, which were shown to be affected after short-term treatment with rapamycin

Low molecular weight inhibitors acts within a very short span of time. A treatment duration of 30 minutes is a long period in which a large number of processes can be influenced (Zisser et al., 2018; H. Bergler, unpublished data). After this interval of rapamycin treatment, the majority of the

assembly factors were released from the pre-ribosomal particles investigated in this study. As described in chapter 1.3, TORC1 influences a variety of cellular processes. One of these processes is the downregulation of transcription. In particular, the downregulation of RiBi regulons could have a great impact on the content of assembly factors in pre-ribosomal complexes.

For this reason, primary effects – the effects that already occurred after 2 minutes of rapamycin treatment – are of great interest.

One of the early effects after rapamycin treatment was the decrease of Nsa2 in Nsa1-particles (Figure 13A). Nsa2 is one of fourteen “B factors”, which are required for the processing of 27SB into 7S and 25.5S pre-rRNA (the 5.8S and 25S precursors) (Woolford and Baserga, 2013). The assembly of B-factors takes place in a hierarchical manner. A subset of B-factors are responsible for the loading of Nsa2 (Talkish et al., 2012), and Nsa2 itself must be present for Nog2 to associate (Biedka et al., 2018; Lebreton et al., 2006; Talkish et al., 2012). Furthermore, data from Biedka et al. suggested an impaired maturation of the peptidyl transferase centre (Biedka et al., 2018), and Lebreton et al. showed an increase of 27SB and a decrease of mature 60S rRNA when Nsa2 is depleted (Lebreton et al., 2006).

As data from this study show, TORC1 influences ribosomal biogenesis at a very early stage. One effect was the decrease of 27SB pre-rRNA (Figure 9). At the remaining 27SB rRNA fraction, Nsa1 was found to be trapped (Figure 13C). Since Nsa2 levels had already decreased after a short treatment period with rapamycin, it is possible that TORC1 inactivation also affects the C₂ cleavage of the remaining 27SB rRNA fraction. In addition, Nsa1-particles exposed to rapamycin for 2 minutes showed decreased levels of Noc3. Noc3 was also found to be absent in most factor B mutants that could not carry out C₂ cleavage (Biedka et al., 2018). Furthermore, an increasing phosphoserine signal, which was migrating in SDS-PAGES similar to Nsa2, was found in the Nog1-TAP strain exposed 30 minutes to rapamycin (Figure 16G; see orange star). However, since TORC1 is a kinase and its inactivation should lead to a decrease of the phosphoserine signal of direct targets, it is likely that TORC1 regulates ribosomal biogenesis factors either via inactivation of additional kinases or via activation of phosphatases. If Nsa2 is indeed a target that is phosphorylated by the TORC1 pathway, the kinase may act via this B factor.

Cic1 is another factor that was noticeably decreased in Nsa1-particles after short-term treatment with rapamycin (Figure 13A). Cic1 interacts directly with ITS2 (Wu et al., 2017) and seems to be involved in the A₂ processing pathway, as inactivation of Cic1 also results in the accumulation of 23S rRNA (Fatica et al., 2003). Thus, it is conceivable that rRNA processing could be influenced via Cic1.

Among the fast effects in Nog1-particles are the decrease in levels of Noc1 and the increase in levels of Noc3 (Figure 14C), although these results should be reproduced. Since several assembly factors (including Nog1, Nog2, Nop7 and Rlp24) accumulate in the nucleolus under rapamycin treatment (Honma et al., 2006; Reiter et al., 2011), and Noc1 is necessary for intranuclear transport (Milkereit et al., 2001), this may be related. The accumulation of Noc3 can be explained by the possibility that the decrease of Noc1 releases several binding sites at the binding partner Noc2 (whose level did not change after 2 minutes of drug treatment), which could then be bound by Noc3. Alternatively, a significant later particle accumulates after rapamycin treatment.

Rok1 is one of a number of Nop58- and Noc2-co-purified factors, which displayed notably decreased levels after only 2 minutes of rapamycin treatment (Figure 8 and 11A). In contrast to other particle-bound proteins, however, the protein levels of Rok1 increased again after prolonged exposure to rapamycin in early nucleolar particles. This was also true for the 90S factor Sof1 in Noc2-particles treated with rapamycin (11A), suggesting that the blockade caused by TORC1 occurs after association of Rok1 and Sof1 in the SSU processome.

Rok1 is only incorporated into pre-ribosomes that are already associated with Rrp5 with the SSU processome (Vos et al., 2004). Rrp5 is one of the few assembly factors necessary for the maturation of the 40S as well as the 60S subunits (Venema and Tollervey, 1996). Rrp5 molecules still associated with 43S-particles after A₂ cleavage must be released in order to depart with 66S-particles. This in turn requires the ATP hydrolysis activity of Rok1 (Khoshnevis et al., 2016). The decrease in Rok1 levels could therefore lead to an accumulation of Rrp5 in pre-40S ribosomes and to a deficiency of Rrp5 in pre-60S ribosomes. The Rrp5 entrapment in pre-40S particles also results in the accumulation of the snoRNA snR30 (Khoshnevis et al., 2016). On the other hand, a lack of Rrp5 in the SSU processome could also have been caused the decrease in Rok1 levels. In order to determine whether Rok1 deficiency is involved in Rrp5 entrapment at the pre-40S subunit, it would be interesting to know how Rrp5 levels of early 43S-particles changed after rapamycin treatment. If Rrp5 indeed decreases in 60S pre-ribosomal particles, this could cause a destabilization in the Noc1-Noc2-Rrp5 module.

In view of our data showing Nop1 dropped in Noc2-particles and trapped at 23S pre-rRNA in Nop58-particles upon rapamycin treatment, it is interesting to note that Sof1 has already been found to interact with this box C/D snoRNP protein during nuclear import (Leslie et al., 2004). Furthermore, Sof1 has been shown to be part of a complex, which associates with the U3 snoRNA within the SSU processome (Barandun et al., 2017).

As exemplified above for Rrp5, both deficiency and accumulation of individual assembly factors can affect ribosomal biogenesis. Similarly the accumulation of Erb1, which shows elevated levels in Nog1-

particles after exposure to rapamycin for 2 minutes (Figure 14C), will have pronounced consequences. The release of Erb1 is required for the binding of Nop53 (Klinge and Woolford, 2019), which recruits the adaptor protein Mtr4 to 66S-particles for exosome-mediated removal of the ITS2 extensions (Thoms et al., 2015). Another example is Nog2 – the recruitment of which requires the presence of all B factors (Talkish et al., 2012). These are only a few of many assembly factors, which, through their absence or entrapment, contribute to the instability of pre-ribosomal complexes. In this respect, the changes brought about at several maturation stages by inhibition of TORC1 through rapamycin treatment will have pronounced consequences on the ribosome biogenesis pathway, finally resulting in redirecting the pathway to 23S pre-rRNA accumulation.

5 References

- Adami, A., García-Alvarez, B., Arias-Palomo, E., Barford, D., and Llorca, O. (2007). Structure of TOR and its complex with KOG1. *Mol. Cell* 27, 509–516.
- Barandun, J., Chaker-Margot, M., Hunziker, M., Molloy, K.R., Chait, B.T., and Klinge, S. (2017). The complete structure of the small-subunit processome. *Nat. Struct. Mol. Biol.* 24, 944–953.
- Barbet, N.C., Schneider, U., Helliwell, S.B., Stansfield, I., Tuite, M.F., and Hall, M.N. (1996). TOR controls translation initiation and early G1 progression in yeast. *Mol. Biol. Cell* 7, 25–42.
- Bernstein, K.A., Gallagher, J.E.G., Mitchell, B.M., Granneman, S., and Baserga, S.J. (2004). The small-subunit processome is a ribosome assembly intermediate. *Eukaryotic Cell* 3, 1619–1626.
- Berset, C., Trachsel, H., and Altmann, M. (1998). The TOR (target of rapamycin) signal transduction pathway regulates the stability of translation initiation factor eIF4G in the yeast *Saccharomyces cerevisiae*. *Proc. Natl. Acad. Sci. U.S.A.* 95, 4264–4269.
- Biedka, S., Micic, J., Wilson, D., Brown, H., Diorio-Toth, L., and Woolford, J.L. (2018). Hierarchical recruitment of ribosomal proteins and assembly factors remodels nucleolar pre-60S ribosomes. *J Cell Biol* 217, 2503–2518.
- Cherkasova, V.A., and Hinnebusch, A.G. (2003). Translational control by TOR and TAP42 through dephosphorylation of eIF2alpha kinase GCN2. *Genes Dev.* 17, 859–872.
- Claypool, J.A., French, S.L., Johzuka, K., Eliason, K., Vu, L., Dodd, J.A., Beyer, A.L., and Nomura, M. (2004). Tor pathway regulates Rrn3p-dependent recruitment of yeast RNA polymerase I to the promoter but does not participate in alteration of the number of active genes. *Mol. Biol. Cell* 15, 946–956.
- Cremonesi, A. (2002). Characterization of the Yeast Rapamycin-sensitive Phosphoproteome. University of Basel.
- de la Cruz, J., Gómez-Herreros, F., Rodríguez-Galán, O., Begley, V., de la Cruz Muñoz-Centeno, M., and Chávez, S. (2018). Feedback regulation of ribosome assembly. *Curr. Genet.* 64, 393–404.
- Dragon, F., Gallagher, J.E.G., Compagnone-Post, P.A., Mitchell, B.M., Porwancher, K.A., Wehner, K.A., Wormsley, S., Settlege, R.E., Shabanowitz, J., Osheim, Y., et al. (2002). A large nucleolar U3 ribonucleoprotein required for 18S ribosomal RNA biogenesis. *Nature* 417, 967–970.
- Fatica, A., Oeffinger, M., Tollervey, D., and Bozzoni, I. (2003). Cic1p/Nsa3p is required for synthesis and nuclear export of 60S ribosomal subunits. *RNA* 9, 1431–1436.
- Fernández-Pevida, A., Kressler, D., and de la Cruz, J. (2015). Processing of preribosomal RNA in *Saccharomyces cerevisiae*. *Wiley Interdiscip Rev RNA* 6, 191–209.
- Grandi, P., Rybin, V., Bassler, J., Petfalski, E., Strauss, D., Marzioch, M., Schäfer, T., Kuster, B., Tschochner, H., Tollervey, D., et al. (2002). 90S pre-ribosomes include the 35S pre-rRNA, the U3 snoRNP, and 40S subunit processing factors but predominantly lack 60S synthesis factors. *Mol. Cell* 10, 105–115.

Heitman, J., Movva, N.R., and Hall, M.N. (1991a). Targets for cell cycle arrest by the immunosuppressant rapamycin in yeast. *Science* 253, 905–909.

Heitman, J., Movva, N.R., Hiestand, P.C., and Hall, M.N. (1991b). FK 506-binding protein proline rotamase is a target for the immunosuppressive agent FK 506 in *Saccharomyces cerevisiae*. *Proc. Natl. Acad. Sci. U.S.A.* 88, 1948–1952.

Helliwell, S.B., Wagner, P., Kunz, J., Deuter-Reinhard, M., Henriquez, R., and Hall, M.N. (1994). TOR1 and TOR2 are structurally and functionally similar but not identical phosphatidylinositol kinase homologues in yeast. *Mol. Biol. Cell* 5, 105–118.

Henras, A., Henry, Y., Bousquet-Antonelli, C., Noaillac-Depeyre, J., Gélugne, J.P., and Caizergues-Ferrer, M. (1998). Nhp2p and Nop10p are essential for the function of H/ACA snoRNPs. *EMBO J.* 17, 7078–7090.

Hierlmeier, T., Merl, J., Sauert, M., Perez-Fernandez, J., Schultz, P., Bruckmann, A., Hamperl, S., Ohmayer, U., Rachel, R., Jacob, A., et al. (2013). Rrp5p, Noc1p and Noc2p form a protein module which is part of early large ribosomal subunit precursors in *S. cerevisiae*. *Nucleic Acids Res.* 41, 1191–1210.

Honma, Y., Kitamura, A., Shioda, R., Maruyama, H., Ozaki, K., Oda, Y., Mini, T., Jenö, P., Maki, Y., Yonezawa, K., et al. (2006). TOR regulates late steps of ribosome maturation in the nucleoplasm via Nog1 in response to nutrients. *EMBO J.* 25, 3832–3842.

Horn, D.M., Mason, S.L., and Karbstein, K. (2011). Rcl1 protein, a novel nuclease for 18 S ribosomal RNA production. *J. Biol. Chem.* 286, 34082–34087.

Huber, A., French, S.L., Tekotte, H., Yerlikaya, S., Stahl, M., Perepelkina, M.P., Tyers, M., Rougemont, J., Beyer, A.L., and Loewith, R. (2011). Sch9 regulates ribosome biogenesis via Stb3, Dot6 and Tod6 and the histone deacetylase complex RPD3L. *EMBO J.* 30, 3052–3064.

Ito, H., Fukuda, Y., Murata, K., and Kimura, A. (1983). Transformation of intact yeast cells treated with alkali cations. *J. Bacteriol.* 153, 163–168.

Kakihara, Y., Makhnevych, T., Zhao, L., Tang, W., and Houry, W.A. (2014). Nutritional status modulates box C/D snoRNP biogenesis by regulated subcellular relocalization of the R2TP complex. *Genome Biol.* 15, 404.

Karuppasamy, M., Kusmider, B., Oliveira, T.M., Gaubitz, C., Prouteau, M., Loewith, R., and Schaffitzel, C. (2017). Cryo-EM structure of *Saccharomyces cerevisiae* target of rapamycin complex 2. *Nat Commun* 8, 1729.

Khoshnevis, S., Askenasy, I., Johnson, M.C., Dattolo, M.D., Young-Erdos, C.L., Stroupe, M.E., and Karbstein, K. (2016). The DEAD-box Protein Rok1 Orchestrates 40S and 60S Ribosome Assembly by Promoting the Release of Rrp5 from Pre-40S Ribosomes to Allow for 60S Maturation. *PLoS Biol.* 14, e1002480.

Klinge, S., and Woolford, J.L. (2019). Ribosome assembly coming into focus. *Nat. Rev. Mol. Cell Biol.* 20, 116–131.

Koltin, Y., Faucette, L., Bergsma, D.J., Levy, M.A., Cafferkey, R., Koser, P.L., Johnson, R.K., and Livi, G.P. (1991). Rapamycin sensitivity in *Saccharomyces cerevisiae* is mediated by a peptidyl-prolyl cis-trans isomerase related to human FK506-binding protein. *Mol. Cell. Biol.* 11, 1718–1723.

- Konikkat, S., and Woolford, J.L. (2017). Principles of 60S ribosomal subunit assembly emerging from recent studies in yeast. *Biochem. J.* *474*, 195–214.
- Kos, M., and Tollervey, D. (2010). Yeast pre-rRNA processing and modification occur cotranscriptionally. *Mol. Cell* *37*, 809–820.
- Kos-Braun, I.C., Jung, I., and Koš, M. (2017). Tor1 and CK2 kinases control a switch between alternative ribosome biogenesis pathways in a growth-dependent manner. *PLoS Biol.* *15*, e2000245.
- Kressler, D., Roser, D., Pertschy, B., and Hurt, E. (2008). The AAA ATPase Rix7 powers progression of ribosome biogenesis by stripping Nsa1 from pre-60S particles. *J. Cell Biol.* *181*, 935–944.
- Kressler, D., Hurt, E., and Bassler, J. (2010). Driving ribosome assembly. *Biochim. Biophys. Acta* *1803*, 673–683.
- Lafontaine, D.L., and Tollervey, D. (1999). Nop58p is a common component of the box C+D snoRNPs that is required for snoRNA stability. *RNA* *5*, 455–467.
- Lafontaine, D.L., and Tollervey, D. (2000). Synthesis and assembly of the box C+D small nucleolar RNPs. *Mol. Cell. Biol.* *20*, 2650–2659.
- Lebreton, A., Saveanu, C., Decourty, L., Jacquier, A., and Fromont-Racine, M. (2006). Nsa2 is an unstable, conserved factor required for the maturation of 27 SB pre-rRNAs. *J. Biol. Chem.* *281*, 27099–27108.
- Leslie, D.M., Zhang, W., Timney, B.L., Chait, B.T., Rout, M.P., Wozniak, R.W., and Aitchison, J.D. (2004). Characterization of karyopherin cargoes reveals unique mechanisms of Kap121p-mediated nuclear import. *Mol. Cell. Biol.* *24*, 8487–8503.
- Li, H., Tsang, C.K., Watkins, M., Bertram, P.G., and Zheng, X.F.S. (2006). Nutrient regulates Tor1 nuclear localization and association with rDNA promoter. *Nature* *442*, 1058–1061.
- Loewith, R., and Hall, M.N. (2011). Target of rapamycin (TOR) in nutrient signaling and growth control. *Genetics* *189*, 1177–1201.
- Loewith, R., Jacinto, E., Wullschleger, S., Lorberg, A., Crespo, J.L., Bonenfant, D., Oppliger, W., Jenoe, P., and Hall, M.N. (2002). Two TOR complexes, only one of which is rapamycin sensitive, have distinct roles in cell growth control. *Mol. Cell* *10*, 457–468.
- Lorenz, M.C., and Heitman, J. (1995). TOR mutations confer rapamycin resistance by preventing interaction with FKBP12-rapamycin. *J. Biol. Chem.* *270*, 27531–27537.
- Lygerou, Z., Allmang, C., Tollervey, D., and Séraphin, B. (1996). Accurate processing of a eukaryotic precursor ribosomal RNA by ribonuclease MRP in vitro. *Science* *272*, 268–270.
- Milkereit, P., Gadal, O., Podtelejnikov, A., Trumtel, S., Gas, N., Petfalski, E., Tollervey, D., Mann, M., Hurt, E., and Tschochner, H. (2001). Maturation and intranuclear transport of pre-ribosomes requires Noc proteins. *Cell* *105*, 499–509.
- Nissan, T.A., Bassler, J., Petfalski, E., Tollervey, D., and Hurt, E. (2002). 60S pre-ribosome formation viewed from assembly in the nucleolus until export to the cytoplasm. *EMBO J.* *21*, 5539–5547.

- Oficjalska-Pham, D., Harismendy, O., Smagowicz, W.J., Gonzalez de Peredo, A., Boguta, M., Sentenac, A., and Lefebvre, O. (2006). General repression of RNA polymerase III transcription is triggered by protein phosphatase type 2A-mediated dephosphorylation of Maf1. *Mol. Cell* *22*, 623–632.
- Osheim, Y.N., French, S.L., Keck, K.M., Champion, E.A., Spasov, K., Dragon, F., Baserga, S.J., and Beyer, A.L. (2004). Pre-18S ribosomal RNA is structurally compacted into the SSU processome prior to being cleaved from nascent transcripts in *Saccharomyces cerevisiae*. *Mol. Cell* *16*, 943–954.
- Philippi, A., Steinbauer, R., Reiter, A., Fath, S., Leger-Silvestre, I., Milkereit, P., Griesenbeck, J., and Tschochner, H. (2010). TOR-dependent reduction in the expression level of Rrn3p lowers the activity of the yeast RNA Pol I machinery, but does not account for the strong inhibition of rRNA production. *Nucleic Acids Res.* *38*, 5315–5326.
- Powers, T., and Walter, P. (1999). Regulation of ribosome biogenesis by the rapamycin-sensitive TOR-signaling pathway in *Saccharomyces cerevisiae*. *Mol. Biol. Cell* *10*, 987–1000.
- Puig, O., Caspary, F., Rigaut, G., Rutz, B., Bouveret, E., Bragado-Nilsson, E., Wilm, M., and Séraphin, B. (2001). The tandem affinity purification (TAP) method: a general procedure of protein complex purification. *Methods* *24*, 218–229.
- Reinke, A., Anderson, S., McCaffery, J.M., Yates, J., Aronova, S., Chu, S., Fairclough, S., Iverson, C., Wedaman, K.P., and Powers, T. (2004). TOR complex 1 includes a novel component, Tco89p (YPL180w), and cooperates with Ssd1p to maintain cellular integrity in *Saccharomyces cerevisiae*. *J. Biol. Chem.* *279*, 14752–14762.
- Reiter, A., Steinbauer, R., Philippi, A., Gerber, J., Tschochner, H., Milkereit, P., and Griesenbeck, J. (2011). Reduction in ribosomal protein synthesis is sufficient to explain major effects on ribosome production after short-term TOR inactivation in *Saccharomyces cerevisiae*. *Mol. Cell. Biol.* *31*, 803–817.
- Sardana, R., White, J.P., and Johnson, A.W. (2013). The rRNA methyltransferase Bud23 shows functional interaction with components of the SSU processome and RNase MRP. *RNA* *19*, 828–840.
- Sardana, R., Liu, X., Granneman, S., Zhu, J., Gill, M., Papoulas, O., Marcotte, E.M., Tollervey, D., Correll, C.C., and Johnson, A.W. (2015). The DEAH-box helicase Dhr1 dissociates U3 from the pre-rRNA to promote formation of the central pseudoknot. *PLoS Biol.* *13*, e1002083.
- Saveanu, C., Namane, A., Gleizes, P.-E., Lebreton, A., Rousselle, J.-C., Noaillic-Depeyre, J., Gas, N., Jacquier, A., and Fromont-Racine, M. (2003). Sequential protein association with nascent 60S ribosomal particles. *Mol. Cell. Biol.* *23*, 4449–4460.
- Schimmang, T., Tollervey, D., Kern, H., Frank, R., and Hurt, E.C. (1989). A yeast nucleolar protein related to mammalian fibrillarin is associated with small nucleolar RNA and is essential for viability. *EMBO J.* *8*, 4015–4024.
- Stan, R., McLaughlin, M.M., Cafferkey, R., Johnson, R.K., Rosenberg, M., and Livi, G.P. (1994). Interaction between FKBP12-rapamycin and TOR involves a conserved serine residue. *J. Biol. Chem.* *269*, 32027–32030.
- Takahara, T., and Maeda, T. (2012). Transient sequestration of TORC1 into stress granules during heat stress. *Mol. Cell* *47*, 242–252.

- Talkish, J., Zhang, J., Jakovljevic, J., Horsey, E.W., and Woolford, J.L. (2012). Hierarchical recruitment into nascent ribosomes of assembly factors required for 27SB pre-rRNA processing in *Saccharomyces cerevisiae*. *Nucleic Acids Res.* *40*, 8646–8661.
- Talkish, J., Biedka, S., Jakovljevic, J., Zhang, J., Tang, L., Strahler, J.R., Andrews, P.C., Maddock, J.R., and Woolford, J.L. (2016). Disruption of ribosome assembly in yeast blocks cotranscriptional pre-rRNA processing and affects the global hierarchy of ribosome biogenesis. *RNA* *22*, 852–866.
- Thoms, M., Thomson, E., Baßler, J., Gnädig, M., Griesel, S., and Hurt, E. (2015). The Exosome Is Recruited to RNA Substrates through Specific Adaptor Proteins. *Cell* *162*, 1029–1038.
- Torreira, E., Louro, J.A., Pazos, I., González-Polo, N., Gil-Carton, D., Duran, A.G., Tosi, S., Gallego, O., Calvo, O., and Fernández-Tornero, C. (2017). The dynamic assembly of distinct RNA polymerase I complexes modulates rDNA transcription. *Elife* *6*.
- Vannini, A., Ringel, R., Kusser, A.G., Berninghausen, O., Kassavetis, G.A., and Cramer, P. (2010). Molecular basis of RNA polymerase III transcription repression by Maf1. *Cell* *143*, 59–70.
- Vanrobays, E., Leplus, A., Osheim, Y.N., Beyer, A.L., Wacheul, L., and Lafontaine, D.L.J. (2008). TOR regulates the subcellular distribution of DIM2, a KH domain protein required for cotranscriptional ribosome assembly and pre-40S ribosome export. *RNA* *14*, 2061–2073.
- Venema, J., and Tollervey, D. (1996). RRP5 is required for formation of both 18S and 5.8S rRNA in yeast. *EMBO J.* *15*, 5701–5714.
- Vos, H.R., Bax, R., Faber, A.W., Vos, J.C., and Raué, H.A. (2004). U3 snoRNP and Rrp5p associate independently with *Saccharomyces cerevisiae* 35S pre-rRNA, but Rrp5p is essential for association of Rok1p. *Nucleic Acids Res.* *32*, 5827–5833.
- Warner, J.R. (1999). The economics of ribosome biosynthesis in yeast. *Trends Biochem. Sci.* *24*, 437–440.
- Watkins, N.J., Ségault, V., Charpentier, B., Nottrott, S., Fabrizio, P., Bachi, A., Wilm, M., Rosbash, M., Branlant, C., and Lührmann, R. (2000). A common core RNP structure shared between the small nuclear box C/D RNPs and the spliceosomal U4 snRNP. *Cell* *103*, 457–466.
- Wei, Y., and Zheng, X.F.S. (2009). Sch9 partially mediates TORC1 signaling to control ribosomal RNA synthesis. *Cell Cycle* *8*, 4085–4090.
- Wei, Y., Tsang, C.K., and Zheng, X.F.S. (2009). Mechanisms of regulation of RNA polymerase III-dependent transcription by TORC1. *EMBO J.* *28*, 2220–2230.
- Wells, G.R., Weichmann, F., Colvin, D., Sloan, K.E., Kudla, G., Tollervey, D., Watkins, N.J., and Schneider, C. (2016). The PIN domain endonuclease Utp24 cleaves pre-ribosomal RNA at two coupled sites in yeast and humans. *Nucleic Acids Res.* *44*, 5399–5409.
- White, J., Li, Z., Sardana, R., Bujnicki, J.M., Marcotte, E.M., and Johnson, A.W. (2008). Bud23 methylates G1575 of 18S rRNA and is required for efficient nuclear export of pre-40S subunits. *Mol. Cell Biol.* *28*, 3151–3161.
- Woolford, J.L., and Baserga, S.J. (2013). Ribosome biogenesis in the yeast *Saccharomyces cerevisiae*. *Genetics* *195*, 643–681.

- Wu, P., Brockenbrough, J.S., Metcalfe, A.C., Chen, S., and Aris, J.P. (1998). Nop5p is a small nucleolar ribonucleoprotein component required for pre-18 S rRNA processing in yeast. *J. Biol. Chem.* *273*, 16453–16463.
- Wu, S., Tan, D., Woolford, J.L., Dong, M.-Q., and Gao, N. (2017). Atomic modeling of the ITS2 ribosome assembly subcomplex from cryo-EM together with mass spectrometry-identified protein-protein crosslinks. *Protein Sci.* *26*, 103–112.
- Yoo, Y.J., Kim, H., Park, S.R., and Yoon, Y.J. (2017). An overview of rapamycin: from discovery to future perspectives. *J. Ind. Microbiol. Biotechnol.* *44*, 537–553.
- Zakalskiy, A., Högenauer, G., Ishikawa, T., Wehrschütz-Sigl, E., Wendler, F., Teis, D., Zisser, G., Steven, A.C., and Bergler, H. (2002). Structural and enzymatic properties of the AAA protein Drg1p from *Saccharomyces cerevisiae*. Decoupling of intracellular function from ATPase activity and hexamerization. *J. Biol. Chem.* *277*, 26788–26795.
- Zaragoza, D., Ghavidel, A., Heitman, J., and Schultz, M.C. (1998). Rapamycin induces the G0 program of transcriptional repression in yeast by interfering with the TOR signaling pathway. *Mol. Cell. Biol.* *18*, 4463–4470.
- Zhang, L., Wu, C., Cai, G., Chen, S., and Ye, K. (2016). Stepwise and dynamic assembly of the earliest precursors of small ribosomal subunits in yeast. *Genes Dev.* *30*, 718–732.
- Zheng, X.F., Florentino, D., Chen, J., Crabtree, G.R., and Schreiber, S.L. (1995). TOR kinase domains are required for two distinct functions, only one of which is inhibited by rapamycin. *Cell* *82*, 121–130.
- Zhu, J., Liu, X., Anjos, M., Correll, C.C., and Johnson, A.W. (2016). Utp14 Recruits and Activates the RNA Helicase Dhr1 To Undock U3 snoRNA from the Preribosome. *Mol. Cell. Biol.* *36*, 965–978.
- Zisser, G., Ohmayer, U., Mauerhofer, C., Mitterer, V., Klein, I., Rechberger, G.N., Wolinski, H., Prattes, M., Pertschy, B., Milkereit, P., et al. (2018). Viewing pre-60S maturation at a minute's timescale. *Nucleic Acids Res.* *46*, 3140–3151.